Accounting for the complex nature of unresolved orography in models

Annelize van Niekerk

Annelize.vanNiekerk@ecmwf.int

Simon Vosper (Met Office)
Miguel Teixeira (Uni. of Reading)

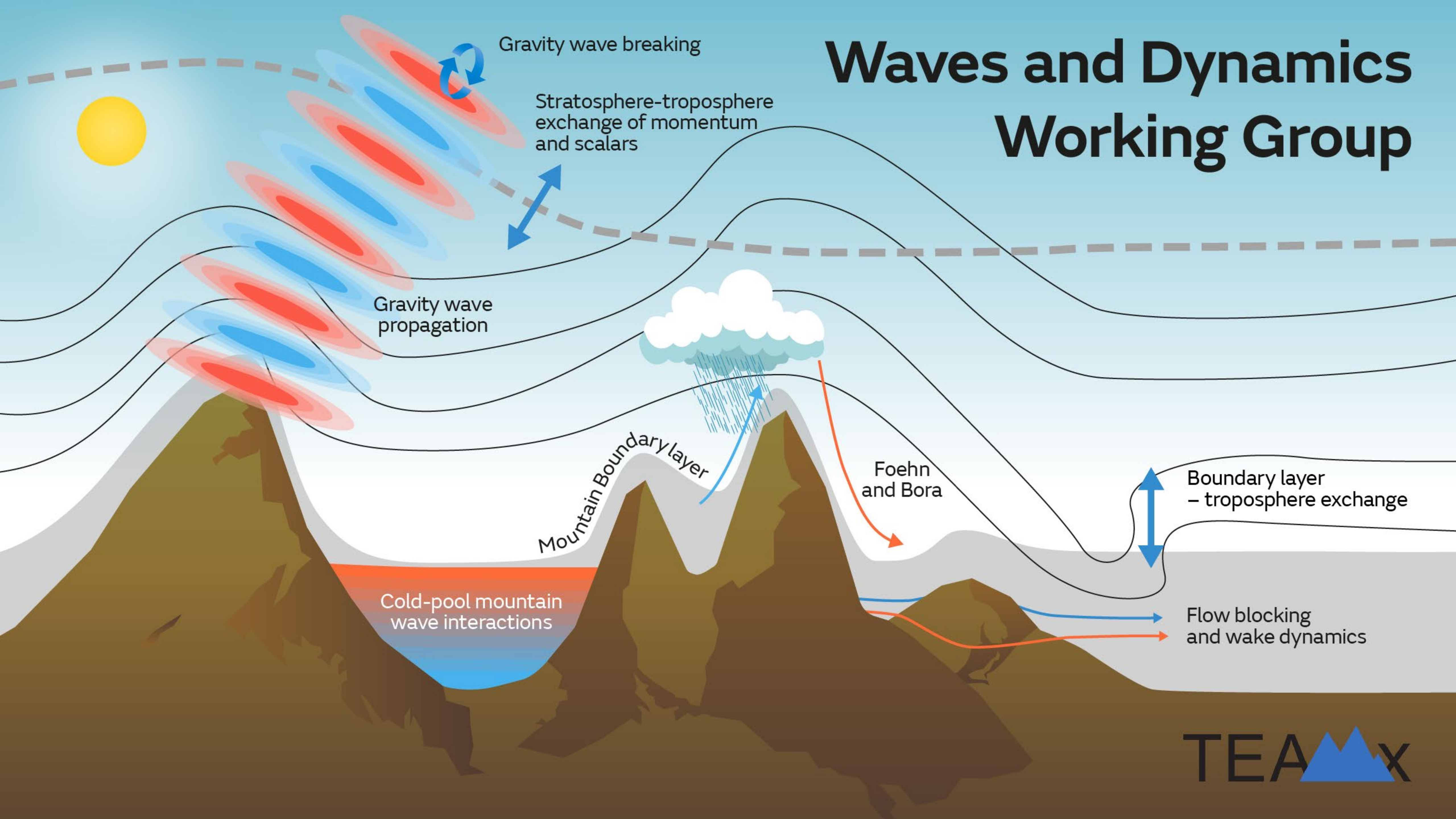
Waves and Dynamics Working Group
Gravity wave breaking
Stratosphere-troposphere exchange of momentum and scalars
Gravity wave propagation
Mountain Boundary layer
Foehn and Bora
Boundary layer – troposphere exchange
Cold-pool mountain wave interactions
Flow blocking and wake dynamics
TEAMx

Waves and Dynamics Working Group

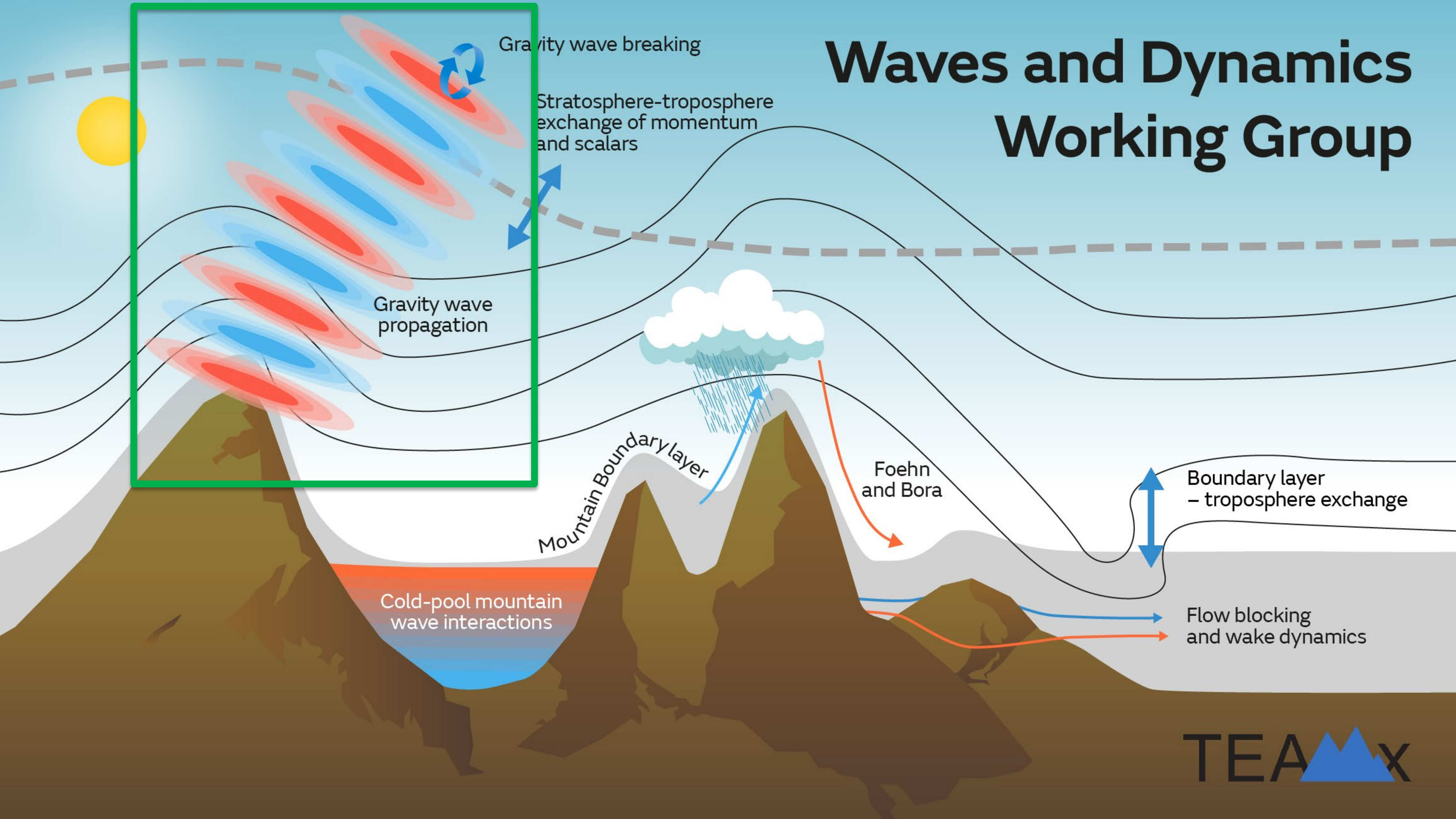

What are orographic gravity waves and what impact do they have?

ECMWF

2.5 km model simulation over the Antarctic Peninsula with Met Office Unified Model

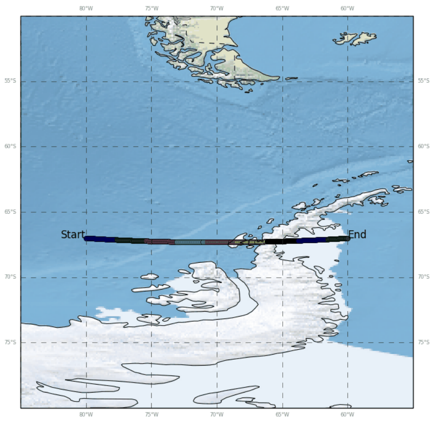

~100 km

Wind speed

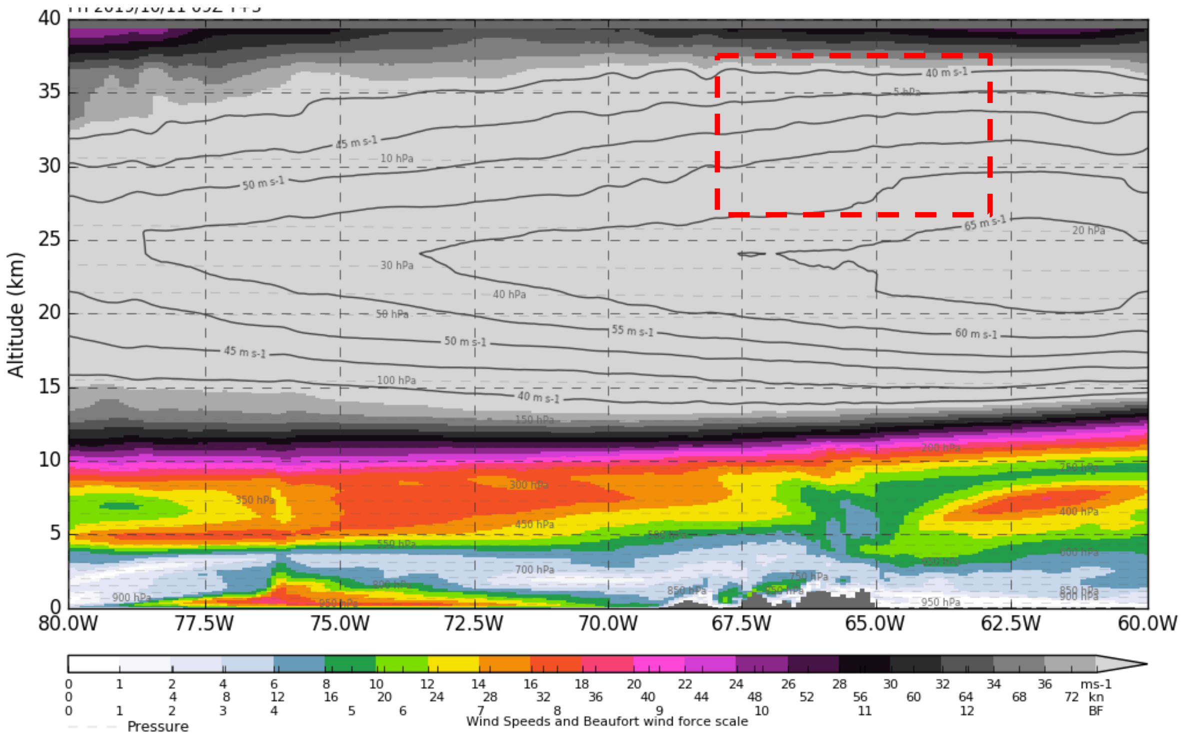

Vertical Velocity

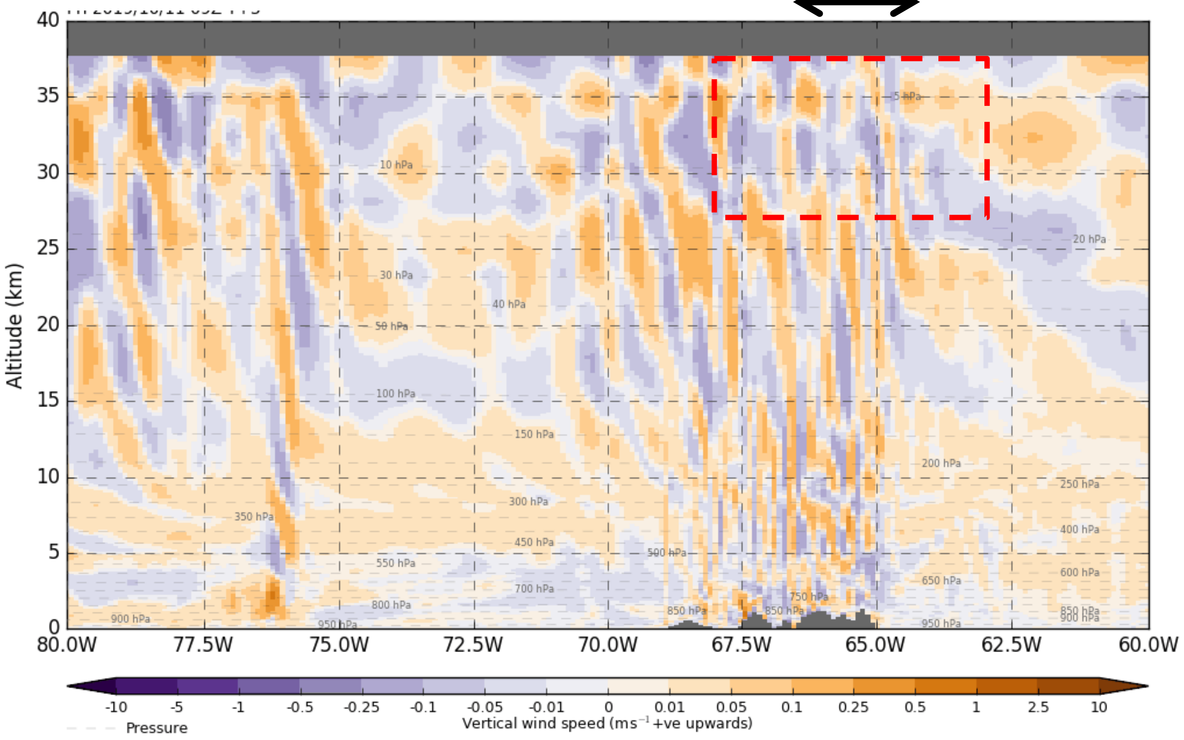

Why do we care about them?

They propagate into the stratosphere

AIRS Satellite Brightness Temperature Perturbations at ~ 40 km

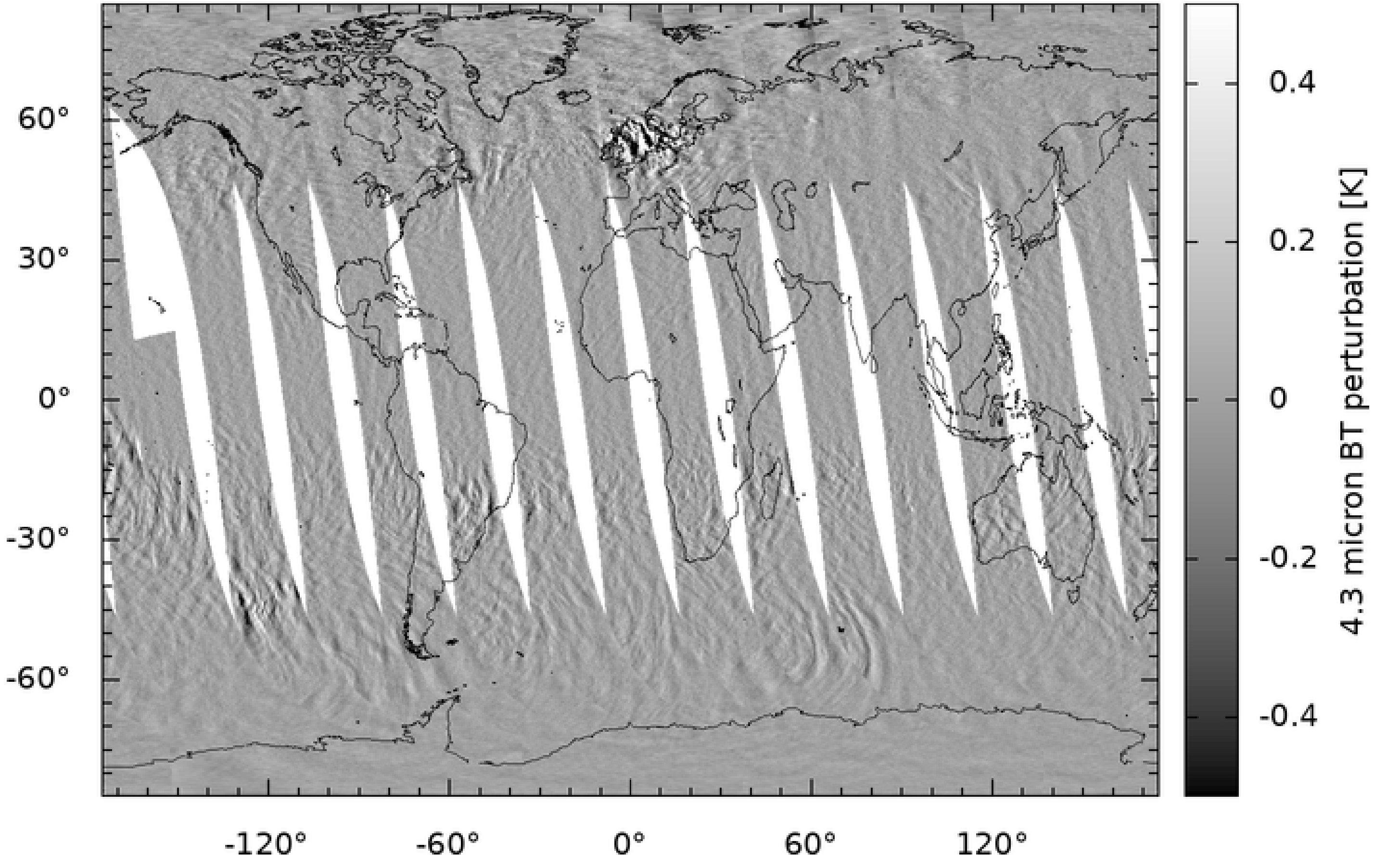

Figure created using https://datapub.fz-juelich.de/slcs/airs/gravity_waves/

They affect Polar Vortex Variability

During Vortex breakdown

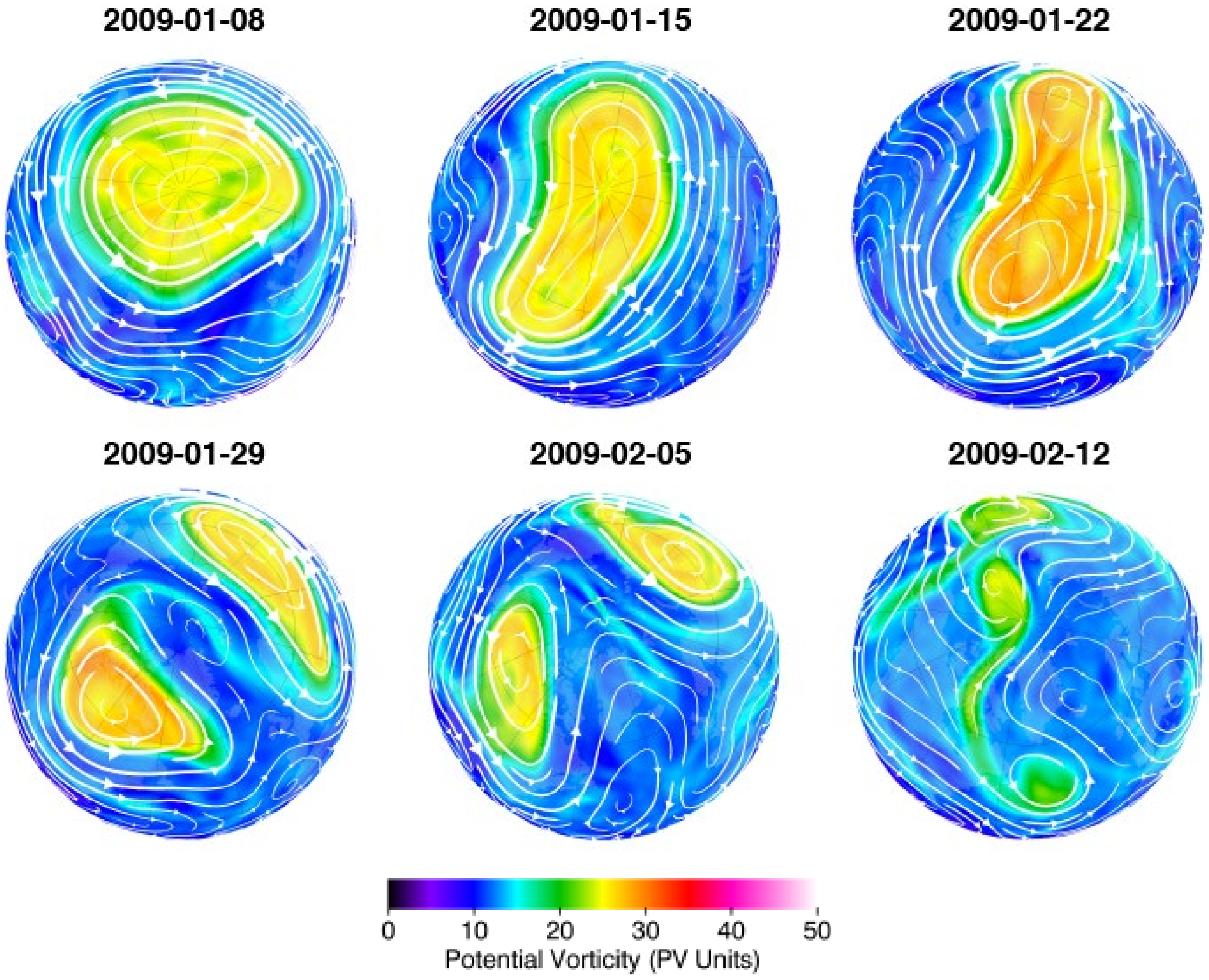

Stratosphere is important for predictability

BBC | annelize | Home | News | Sport | Weather | iPlayer | Sounds

NEWS

Home | Coronavirus | Climate | UK | World | Business | Politics | Tech | Science | Health | Family & Education

World | Africa | Asia | Australia | Europe | Latin America | Middle East | US & Canada

Polar vortex death toll rises to 21 as US cold snap continues

1 February 2019

US polar vortex

Chicago's frozen shoreline

At least 21 people have died in one of the worst cold snaps to hit the US Midwest in decades.

nature > communications earth & environment > articles > article

Article | Open Access | Published: 23 July 2021

Northern hemisphere cold air outbreaks are more likely to be severe during weak polar vortex conditions

Jinlong Huang, Peter Hitchcock, Amanda C. Maycock, Christine M. McKenna & Wenshou Tian

Communications Earth & Environment **2**, Article number: 147 (2021) | Cite this article

Abstract

Severe cold air outbreaks have significant impacts on human health, energy use, agriculture, and transportation. Anomalous behavior of the Arctic stratospheric polar vortex provides an important source of subseasonal-to-seasonal predictability of Northern Hemisphere cold air outbreaks. Here, through reanalysis data for the period 1958–2019 and climate model simulations for preindustrial conditions, we show that weak stratospheric polar vortex conditions increase the risk of severe cold air outbreaks in mid-latitude East Asia by 100%, in contrast to only 40% for moderate cold air outbreaks. Such a disproportionate increase is also found in Europe, with an elevated risk persisting more than three weeks. By analysing the stream of polar cold air mass, we show that the polar vortex affects severe cold air outbreaks by modifying the inter-hemispheric transport of cold air mass. Using a novel method to assess Granger causality, we show that the polar vortex provides predictive information regarding severe cold air outbreaks over multiple regions in the Northern Hemisphere, which may help with mitigating their impact.

How are they represented in models?

They can be explicitly resolved by model dynamics

Momentum

$$\frac{Du}{Dt} = -\frac{uw}{r} - 2\Omega w cos\phi + \frac{uvtan\phi}{r} + 2\Omega sin\phi v - \frac{1}{\rho r cos\phi}\frac{\partial p}{\partial \lambda}$$

$$\frac{Dv}{Dt} = -\frac{vw}{r} - \frac{u^2 tan\phi}{r} - 2\Omega sin\phi u - \frac{1}{\rho r}\frac{\partial p}{\partial \phi}$$

$$\frac{Dw}{Dt} = \frac{(u^2+v^2)}{r} + 2\Omega cos\phi u - g - \frac{1}{\rho}\frac{\partial p}{\partial r}$$

Mass Continuity

$$\frac{\partial \rho}{\partial t} + \nabla \cdot \rho \boldsymbol{u} = 0$$

Thermodynamics

$$\frac{D\theta}{Dt} = \frac{\theta}{T}\frac{\dot{Q}}{c_p}$$

They can be explicitly resolved by model dynamics

Momentum

$$\frac{Du}{Dt} = -\frac{uw}{r} - 2\Omega w cos\phi + \frac{uvtan\phi}{r} + 2\Omega sin\phi v - \frac{1}{\rho r cos\phi}\frac{\partial p}{\partial \lambda}$$

$$\frac{Dv}{Dt} = -\frac{vw}{r} - \frac{u^2 tan\phi}{r} - 2\Omega sin\phi u - \frac{1}{\rho r}\frac{\partial p}{\partial \phi}$$

$$\frac{Dw}{Dt} = \frac{(u^2+v^2)}{r} + 2\Omega cos\phi u - g - \frac{1}{\rho}\frac{\partial p}{\partial r}$$

Inferred temperature variances at 30-40 km altitude

2.5 km UM

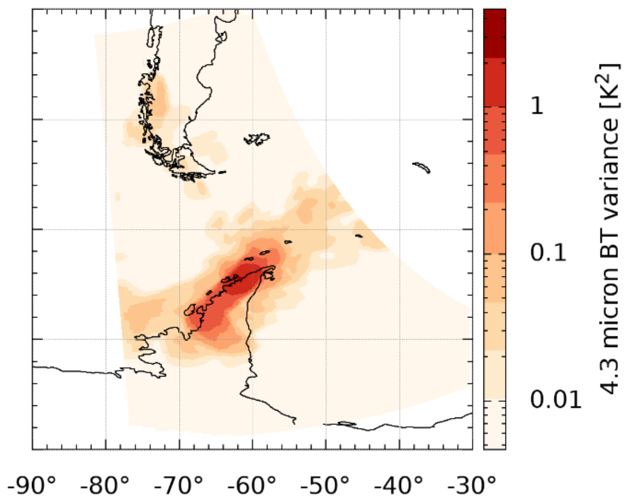

Kruse et al (2021), JAS

Mass Continuity

$$\frac{\partial \rho}{\partial t} + \nabla \cdot \rho \boldsymbol{u} = 0$$

Thermodynamics

$$\frac{D\theta}{Dt} = \frac{\theta}{T}\frac{\dot{Q}}{c_p}$$

They can be explicitly resolved by model dynamics

Momentum

$$\frac{Du}{Dt} = -\frac{uw}{r} - 2\Omega w cos\phi + \frac{uv tan\phi}{r} + 2\Omega sin\phi v - \frac{1}{\rho r cos\phi}\frac{\partial p}{\partial \lambda}$$

$$\frac{Dv}{Dt} = -\frac{vw}{r} - \frac{u^2 tan\phi}{r} - 2\Omega sin\phi u - \frac{1}{\rho r}\frac{\partial p}{\partial \phi}$$

$$\frac{Dw}{Dt} = \frac{(u^2+v^2)}{r} + 2\Omega cos\phi u - g - \frac{1}{\rho}\frac{\partial p}{\partial r}$$

Mass Continuity

$$\frac{\partial \rho}{\partial t} + \nabla \cdot \rho \boldsymbol{u} = 0$$

Thermodynamics

$$\frac{D\theta}{Dt} = \frac{\theta}{T}\frac{\dot{Q}}{c_p}$$

Inferred temperature variances at 30-40 km altitude

AIRS satellite

2.5 km UM

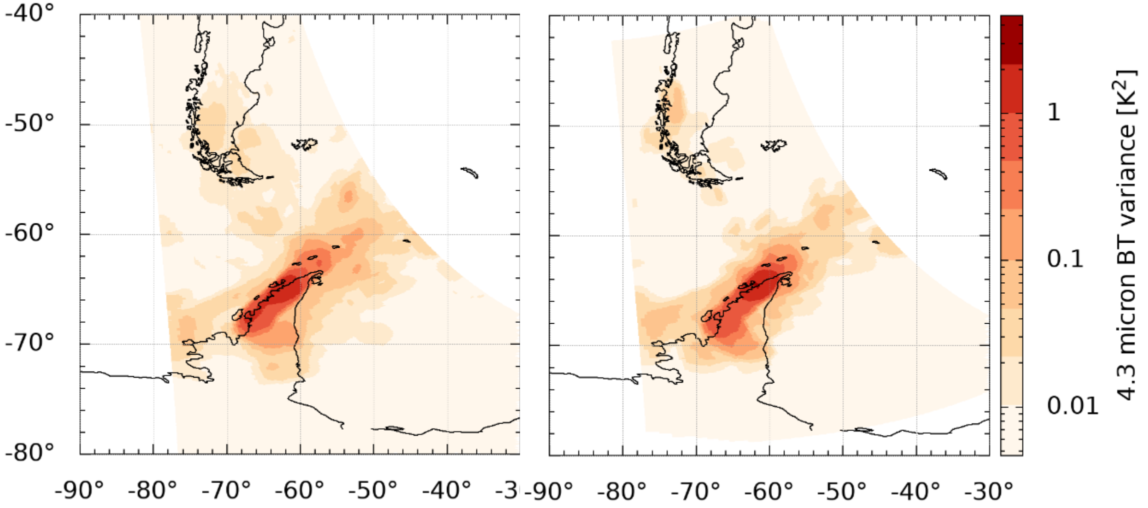

Kruse et al (2021), JAS

They can be explicitly resolved by model dynamics

Momentum

$$\frac{Du}{Dt} = -\frac{uw}{r} - 2\Omega w cos\phi + \frac{uvtan\phi}{r} + 2\Omega sin\phi v - \frac{1}{\rho r cos\phi}\frac{\partial p}{\partial \lambda}$$

$$\frac{Dv}{Dt} = -\frac{vw}{r} - \frac{u^2 tan\phi}{r} - 2\Omega sin\phi u - \frac{1}{\rho r}\frac{\partial p}{\partial}$$

$$\frac{Dw}{Dt} = \frac{(u^2+v^2)}{r} + 2\Omega cos\phi u - g - \frac{1}{\rho}\frac{\partial p}{\partial r}$$

Mass Continuity

$$\frac{\partial \rho}{\partial t} + \nabla \cdot \rho \boldsymbol{u} = 0$$

Thermodynamics

$$\frac{D\theta}{Dt} = \frac{\theta}{T}\frac{\dot{Q}}{c_p}$$

Inferred temperature variances at 30-40 km altitude

AIRS satellite | 2.5 km UM | 9 km ECMWF IFS

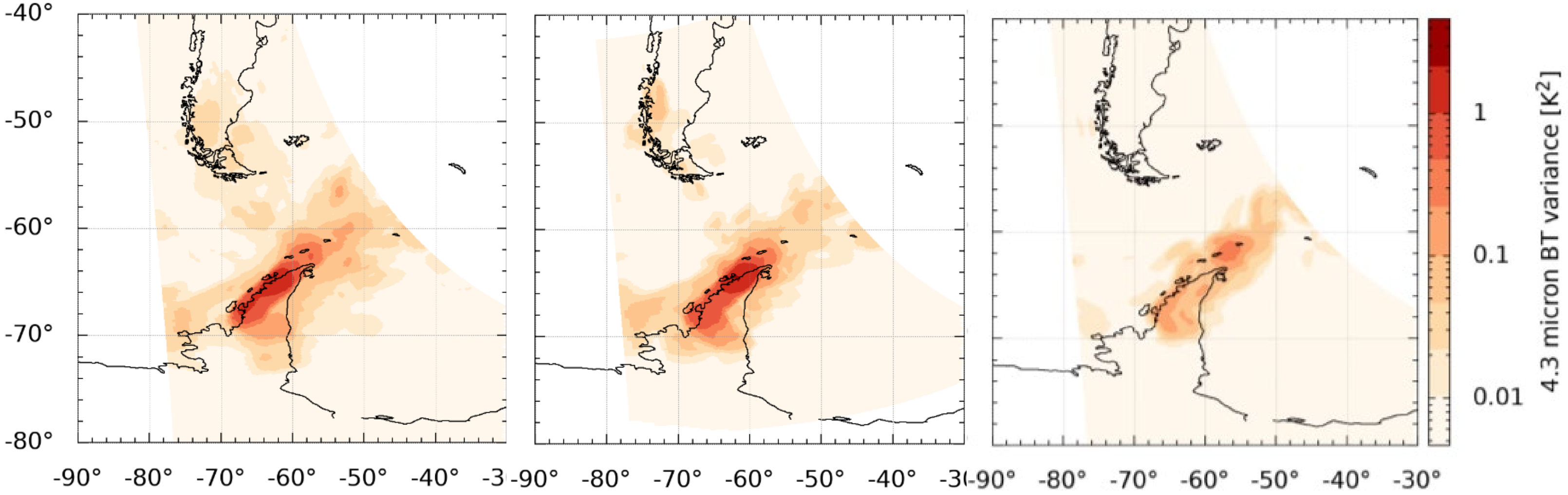

Kruse et al (2021), JAS

They can be explicitly resolved by model dynamics

Momentum

$$\frac{Du}{Dt} = -\frac{uw}{r} - 2\Omega w cos\phi + \frac{uvtan\phi}{r} + 2\Omega sin\phi v - \frac{1}{\rho r cos\phi}\frac{\partial p}{\partial \lambda}$$

$$\frac{Dv}{Dt} = -\frac{vw}{r} - \frac{u^2 tan\phi}{r} - 2\Omega sin\phi u - \frac{1}{\rho r}\frac{\partial p}{\partial \phi}$$

$$\frac{Dw}{Dt} = \frac{(u^2+v^2)}{r} + 2\Omega cos\phi u - g - \frac{1}{\rho}\frac{\partial p}{\partial r}$$

Mass Continuity

$$\frac{\partial \rho}{\partial t} + \nabla \cdot \rho \boldsymbol{u} = 0$$

Thermodynamics

$$\frac{D\theta}{Dt} = \frac{\theta}{T}\frac{\dot{Q}}{c_p}$$

They must also be parametrized

Momentum

$$\frac{Du}{Dt} = -\frac{uw}{r} - 2\Omega w cos\phi + \frac{uvtan\phi}{r} + 2\Omega sin\phi v - \frac{1}{\rho r cos\phi}\frac{\partial p}{\partial \lambda} + F_u$$

$$\frac{Dv}{Dt} = -\frac{vw}{r} - \frac{u^2 tan\phi}{r} - 2\Omega sin\phi u - \frac{1}{\rho r}\frac{\partial p}{\partial \phi} + F_v$$

$$\frac{Dw}{Dt} = \frac{(u^2+v^2)}{r} + 2\Omega cos\phi u - g - \frac{1}{\rho}\frac{\partial p}{\partial r}$$

Mass Continuity

$$\frac{\partial \rho}{\partial t} + \nabla \cdot \rho \boldsymbol{u} = 0$$

Thermodynamics

$$\frac{D\theta}{Dt} = \frac{\theta}{T}\frac{\dot{Q}}{c_p}$$

F_u, F_v= parametrized zonal and meridional wind forcing from gravity waves

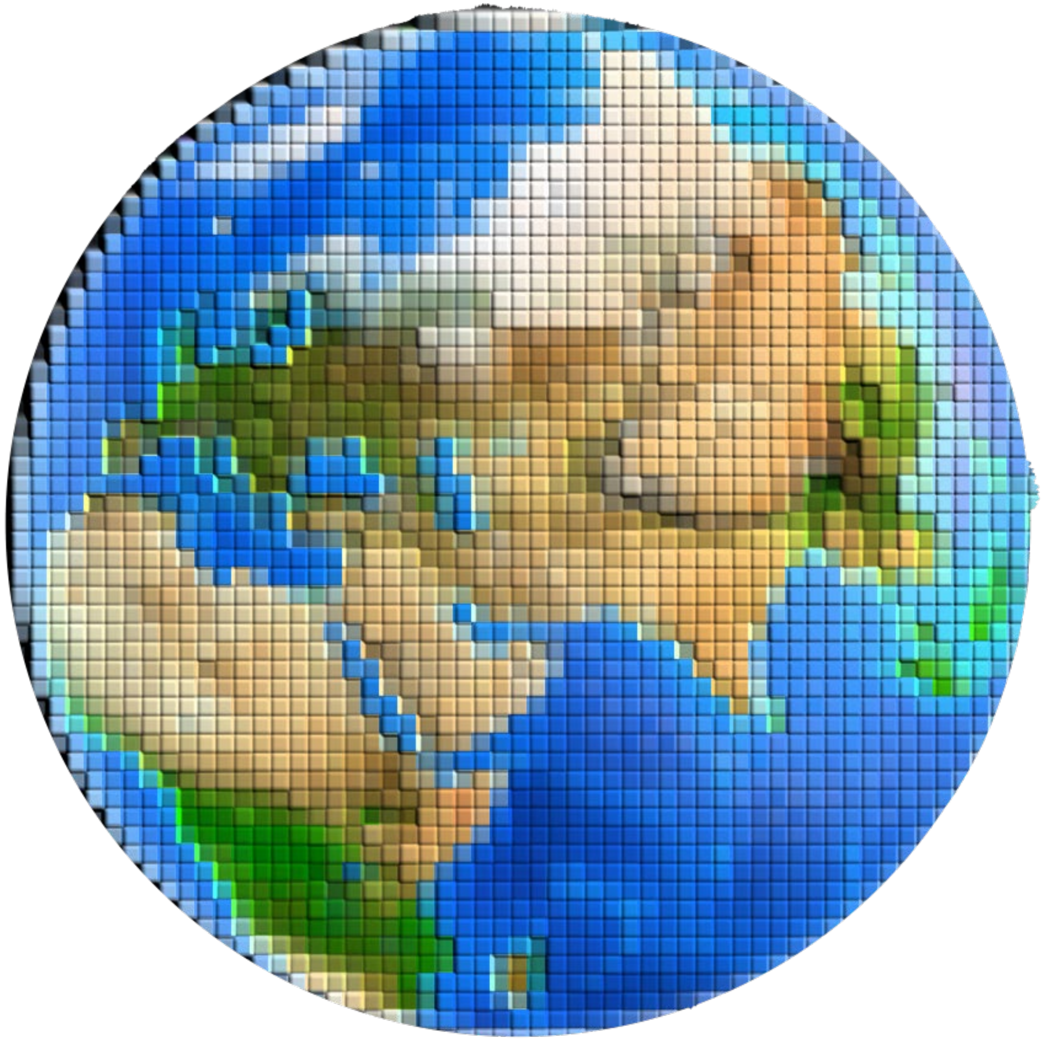

How are they represented in theory?

Their impacts are approximated through simplification

Momentum

$$\frac{Du}{Dt} = -\frac{uw}{r} - 2\Omega w cos\phi + \frac{uvtan\phi}{r} + 2\Omega sin\phi v - \frac{1}{\rho r cos\phi}\frac{\partial p}{\partial \lambda}$$

$$\frac{Dv}{Dt} = -\frac{vw}{r} - \frac{u^2 tan\phi}{r} - 2\Omega sin\phi u - \frac{1}{\rho r}\frac{\partial p}{\partial \phi}$$

$$\frac{Dw}{Dt} = \frac{(u^2+v^2)}{r} + 2\Omega cos\phi u - g - \frac{1}{\rho}\frac{\partial p}{\partial r}$$

Mass Continuity

$$\frac{\partial \rho}{\partial t} + \nabla \cdot \rho \boldsymbol{u} = 0$$

Thermodynamics

$$\frac{D\theta}{Dt} = \frac{\theta}{T}\frac{\dot{Q}}{c_p}$$

Their impacts are approximated through simplification

Momentum

$$\boldsymbol{u} \cdot \nabla u = -\frac{1}{\rho}\frac{\partial p}{\partial x}$$

$$\boldsymbol{u} \cdot \nabla v = -\frac{1}{\rho}\frac{\partial p}{\partial y}$$

$$\frac{\partial p}{\partial z} = -\rho g$$

Mass Continuity

$$\nabla \cdot \rho \boldsymbol{u} = 0$$

Thermodynamics

$$\boldsymbol{u} \cdot \nabla \theta = 0$$

Following assumptions are made:

Cartesian coordinates
No rotation
Adiabatic
Steady state
Hydrostatic equilibrium

Their impacts are approximated through simplification

Momentum

$$U\frac{\partial u'}{\partial x}+V\frac{\partial u'}{\partial y}+w'\frac{\partial U}{\partial z}=-\frac{1}{\rho}\frac{\partial p'}{\partial x}$$

$$U\frac{\partial v'}{\partial x}+V\frac{\partial v'}{\partial y}+w'\frac{\partial V}{\partial z}=-\frac{1}{\rho}\frac{\partial p'}{\partial y}$$

$$\frac{\partial p'}{\partial z}=-\rho g$$

Mass Continuity

$$\frac{\partial u'}{\partial x}+\frac{\partial v'}{\partial y}+\frac{\partial w'}{\partial z}=0$$

Thermodynamics

$$U\frac{\partial \theta'}{\partial x}+V\frac{\partial \theta'}{\partial y}+w'\frac{\partial \Theta}{\partial z}=0$$

Following assumptions are made:

Cartesian coordinates
No rotation
Adiabatic
Steady state
Hydrostatic equilibrium

Linearised : $u=U(z)+u'(x,y,z),\ u'u'\sim 0$

Their impacts are approximated through simplification

Momentum

$$U\frac{\partial u'}{\partial x}+V\frac{\partial u'}{\partial y}+w'\frac{\partial U}{\partial z}=-\frac{1}{\rho}\frac{\partial p'}{\partial x}$$

$$U\frac{\partial v'}{\partial x}+V\frac{\partial v'}{\partial y}+w'\frac{\partial V}{\partial z}=-\frac{1}{\rho}\frac{\partial p'}{\partial y}$$

$$\frac{\partial p'}{\partial z}=-\rho g$$

Mass Continuity

$$\frac{\partial u'}{\partial x}+\frac{\partial v'}{\partial y}+\frac{\partial w'}{\partial z}=0$$

Thermodynamics

$$U\frac{\partial \theta'}{\partial x}+V\frac{\partial \theta'}{\partial y}+w'\frac{\partial \Theta}{\partial z}=0$$

Following assumptions are made:

Cartesian coordinates
No rotation
Adiabatic
Steady state
Hydrostatic equilibrium

Linearised : $u=U(z)+u'(x,y,z),\ u'u'\sim 0$

At the surface the vertical velocity is: $w'(x,y,0)=\boldsymbol{U}\cdot\nabla h$

$\boldsymbol{h}$ = height at the surface

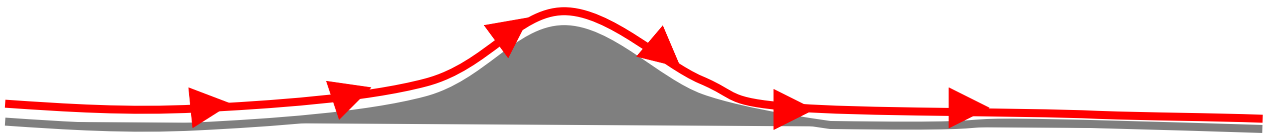

Their impacts are approximated through simplification

Momentum

$$U\,\hat{u}ik + V\,\hat{u}il + \hat{w}\frac{\partial U}{\partial z} = -\frac{1}{\rho}\,\hat{p}ik$$

$$U\,\hat{v}ik + V\,\hat{v}il + \hat{w}\frac{\partial V}{\partial z} = -\frac{1}{\rho}\,\hat{p}il$$

$$\frac{\partial\,\hat{p}}{\partial z} = -\rho g$$

Mass Continuity

$$\hat{u}ik + \hat{v}il + \frac{\partial \hat{w}}{\partial z} = 0$$

Thermodynamics

$$U\,\hat{\theta}ik + V\,\hat{\theta}il + \hat{w}\frac{\partial \Theta}{\partial z} = 0$$

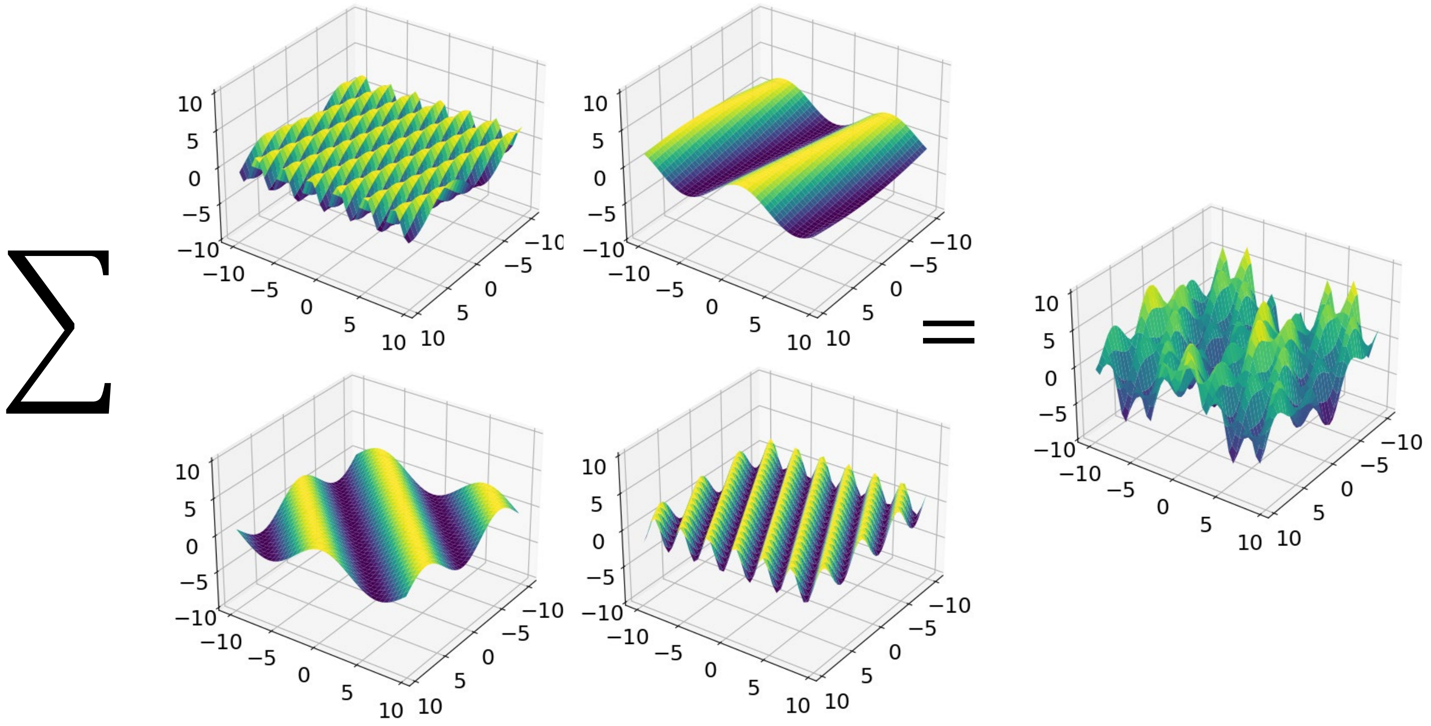

$$h' \sim \int_{-\infty}^{\infty}\int_{-\infty}^{\infty} \hat{h}\,(\cos(kx+ly) + i\sin(kx+ly))\,dk\,dl$$

...

$$w' \sim \int_{-\infty}^{\infty}\int_{-\infty}^{\infty} \hat{w}\,(\cos(kx+ly) + i\sin(kx+ly))\,dk\,dl$$

...

k, l = zonal and meridional wavenumber

Their impacts are approximated through simplification

Momentum

$$U\,\hat{u}ik + V\,\hat{u}il + \hat{w}\frac{\partial U}{\partial z} = -\frac{1}{\rho}\,\hat{p}ik$$

$$U\,\hat{v}ik + V\,\hat{v}il + \hat{w}\frac{\partial V}{\partial z} = -\frac{1}{\rho}\,\hat{p}il$$

$$\frac{\partial\,\hat{p}}{\partial z} = -\rho g$$

Mass Continuity

$$\hat{u}ik + \hat{v}il + \frac{\partial \hat{w}}{\partial z} = 0$$

Thermodynamics

$$U\,\hat{\theta}ik + V\,\hat{\theta}il + \hat{w}\frac{\partial \Theta}{\partial z} = 0$$

$$\frac{d\,(U,V)}{dt} = -\frac{1}{\rho}\frac{\partial}{\partial z}\left(\rho\overline{u'w'}, \rho\overline{v'w'}\right)$$

Assume that vertical momentum flux dominates

Expression for the momentum flux can be derived

Linear hydrostatic gravity wave surface stress in spectral space:

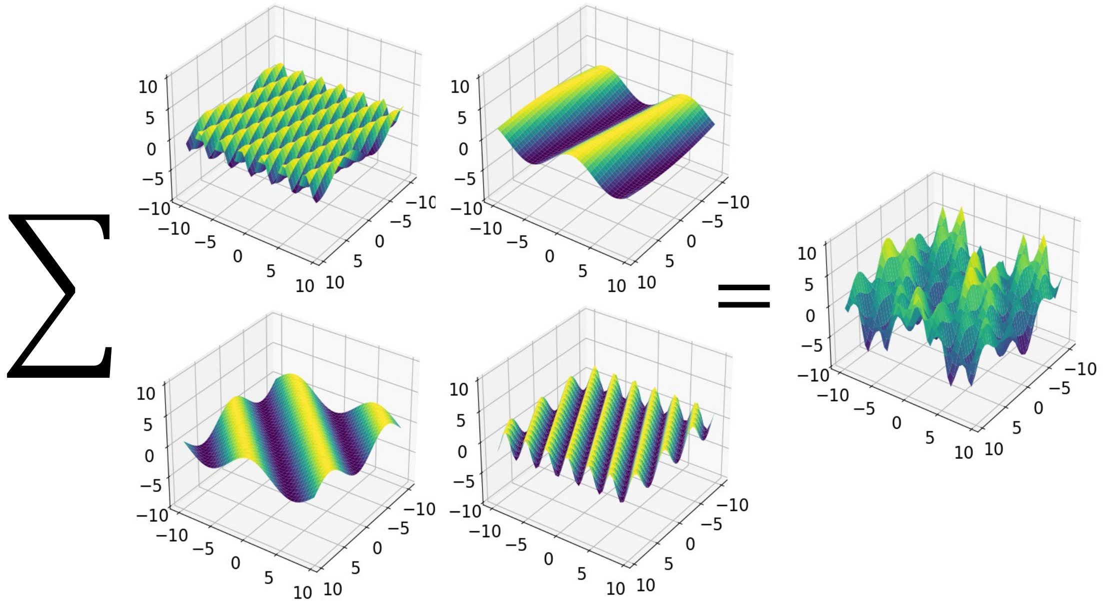

$$\tau_x, \tau_y = \left(\rho\overline{u'w'}, \rho\overline{v'w'}\right)$$

$$= A^{-1}\rho_0 N_o 4\pi^2 \int_{-\infty}^{\infty}\int_{-\infty}^{\infty} \frac{(k,l)}{K}(U_0 k + V_0 l)\left|\hat{h}\right|^2 dk\, dl$$

ρ_0 = Density

N_0 = Stability

k, l = zonal and meridional wavenumber

$K = (k+l)^{\frac{1}{2}}$

A = Area

$U_0 k + V_0 l$ = Surface wind

$\left|\hat{h}\right|$ = Fourier transform of mountain height

How are they parametrized in models?

Mountains are assumed to be ellipses

Grid-box

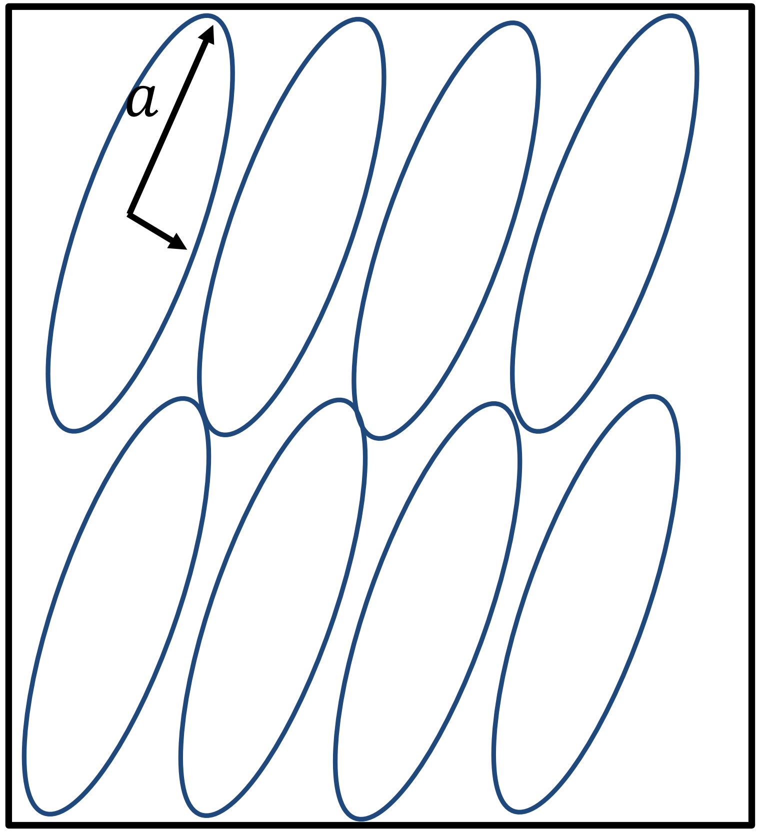

Linear hydrostatic gravity wave surface stress:

$$\tau_x, \tau_y = A^{-1}\rho_0 \int_{-\infty}^{\infty}\int_{-\infty}^{\infty}(u', v')w'dxdy$$

$$= A^{-1}\rho_0 N_o 4\pi^2 \int_{-\infty}^{\infty}\int_{-\infty}^{\infty}\frac{k,l}{K}(U_0 k + V_0 l)\left|\hat{h}\right|^2 dk\, dl$$

$\left|\hat{h}\right|$ = Fourier transform of surface height

Mountains are assumed to be ellipses

Grid-box

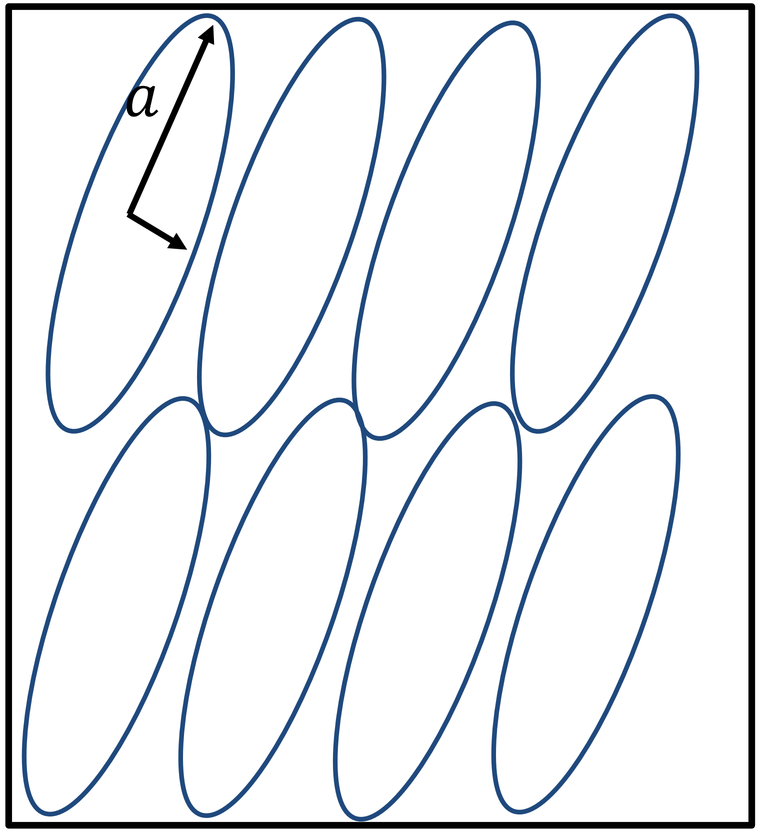

Linear hydrostatic gravity wave surface stress:

$$\tau_x, \tau_y = A^{-1}\rho_0 \int_{-\infty}^{\infty}\int_{-\infty}^{\infty}(u', v')w'dxdy$$

$$= A^{-1}\rho_0 N_o 4\pi^2 \int_{-\infty}^{\infty}\int_{-\infty}^{\infty}\frac{k,l}{K}(U_0k + V_0l)\left|\hat{h}\right|^2 dk\, dl$$

$\left|\hat{h}\right|$ = Fourier transform of surface height

Assume elliptical mountains (Lott and Miller 1997, Phillips 1984):

$$\tau_x, \tau_y = G\rho N \frac{1}{4a} h_{eff}^2 (U\vec{D})$$

Mountains are assumed to be ellipses

Grid-box

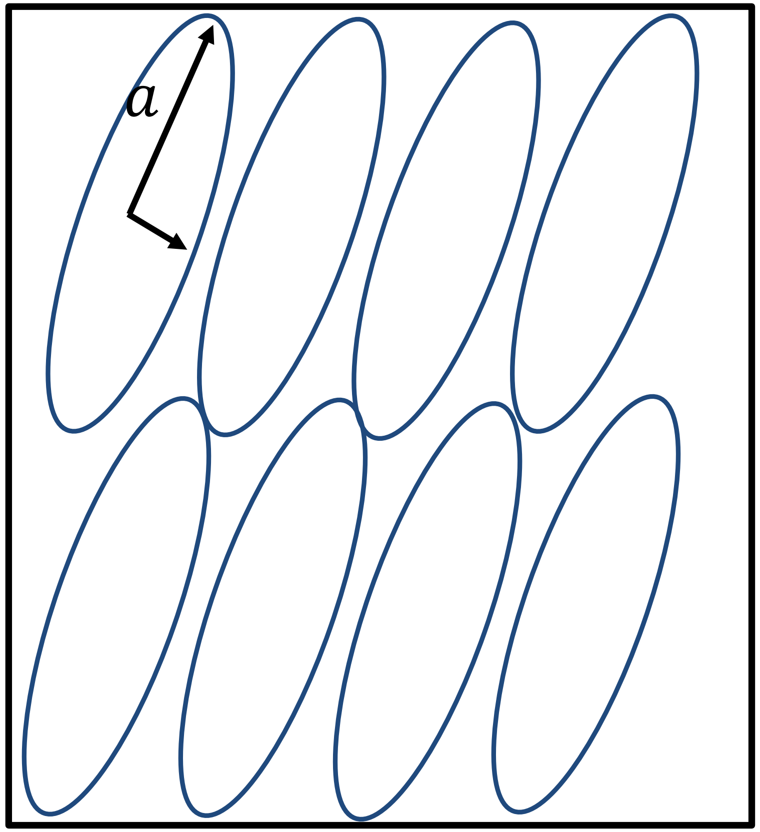

Linear hydrostatic gravity wave surface stress:

$$\tau_x, \tau_y = A^{-1}\rho_0 \int_{-\infty}^{\infty}\int_{-\infty}^{\infty} (u', v')w' dxdy$$

$$= A^{-1}\rho_0 N_o 4\pi^2 \int_{-\infty}^{\infty}\int_{-\infty}^{\infty} \frac{k,l}{K}(U_0 k + V_0 l)\left|\hat{h}\right|^2 dk\, dl$$

$\left|\hat{h}\right|$ = Fourier transform of surface height

Assume elliptical mountains (Lott and Miller 1997, Phillips 1984):

$$\tau_x, \tau_y = G\rho N \frac{1}{4a} h_{eff}^2 (U\vec{D})$$

Mountain half-width

Effective mountain height

Mountain anisotropy

$$\mathrm{h}_{eff} = min\left(h, \frac{U}{NF_c}\right)$$

Accounting for weak winds or high stability

Mountain half-width

Effective mountain height

Mountain anisotropy

$$\tau_x, \tau_y = G\rho N \frac{1}{4a} h_{eff}^2 (U\vec{D})$$

$$\mathrm{h}_{eff} = min\left(h, \frac{U}{NF_c}\right)$$

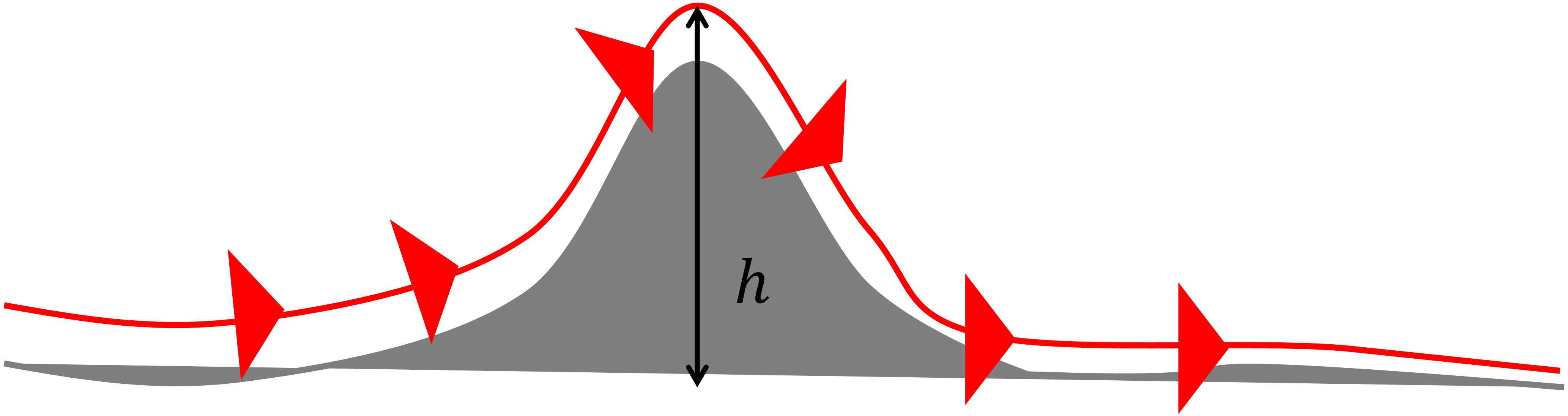

Accounting for weak winds or high stability

Mountain half-width

Effective mountain height

Mountain anisotropy

$$\tau_x, \tau_y = G\rho N \frac{1}{4a} h_{eff}^2 (U\vec{D})$$

$$\mathrm{h}_{eff} = min\left(h, \frac{U}{NF_c}\right)$$

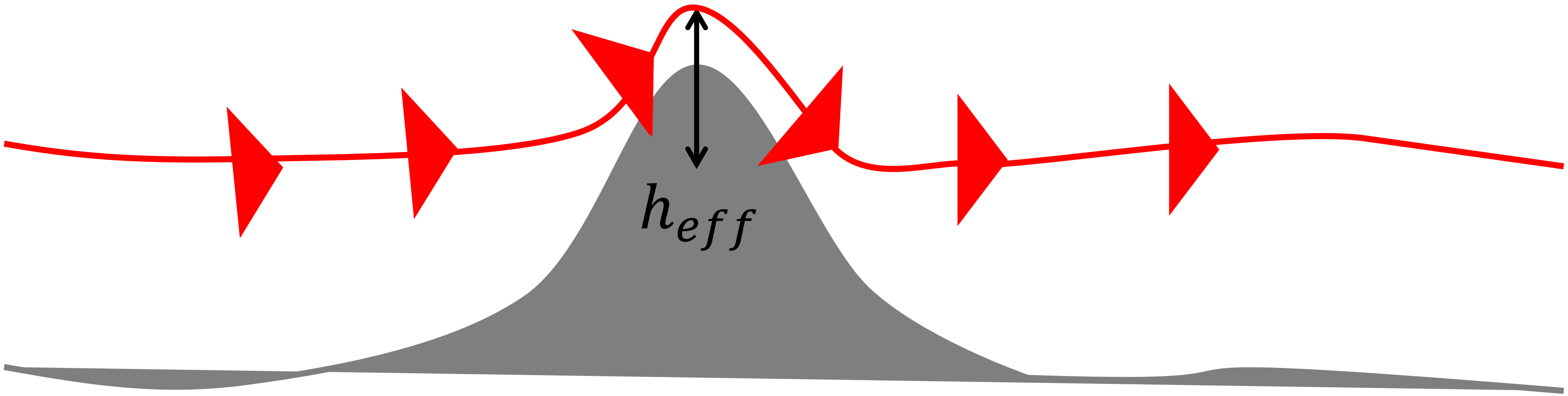

ECMWF

How scale-aware is the current parametrization?

ECMWF

Total momentum flux should be constant across resolutions

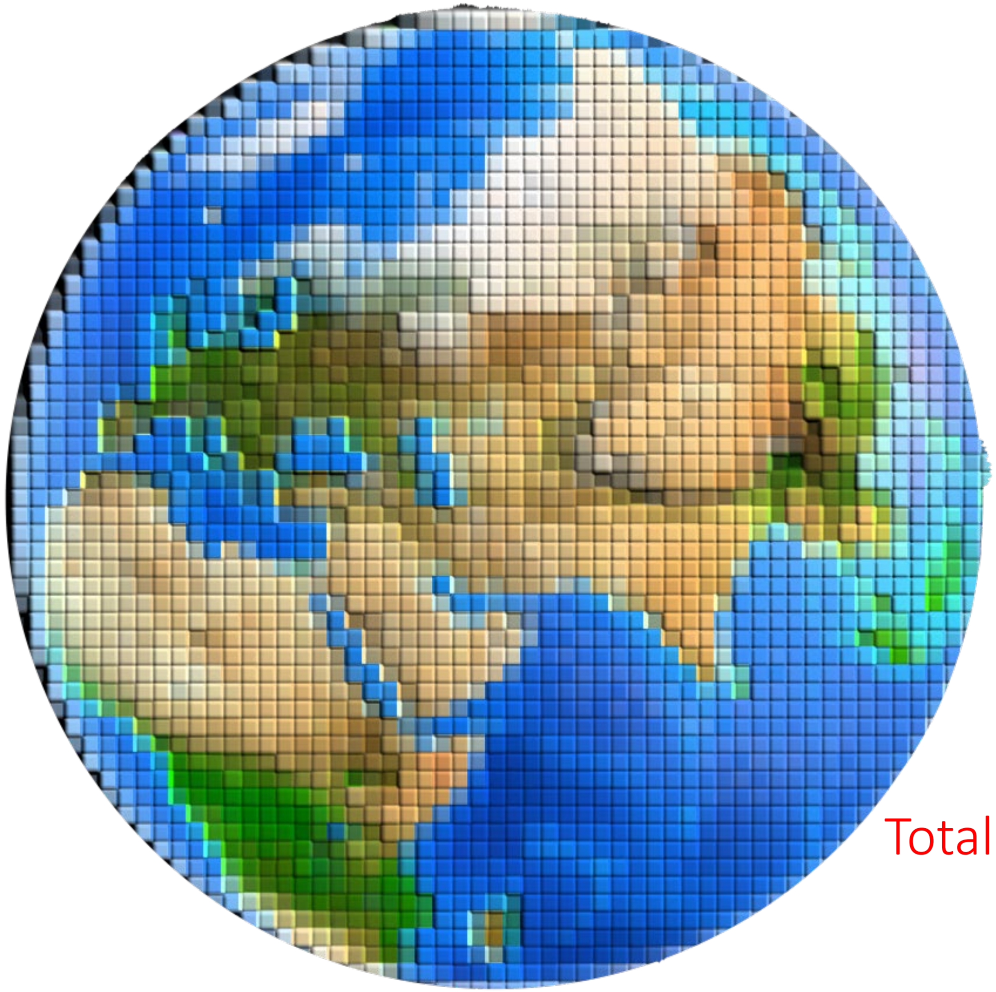

Run global UM model initialised from ECMWF analysis at grid-spacings of:

N96 (~130 km) Climate

$$\tau_{Tot} = \tau_{RES} + \tau_{GWD}$$

Total momentum flux

Resolved momentum flux: $\overline{\rho u' w'}$

Parametrized momentum flux

Total momentum flux should be constant across resolutions

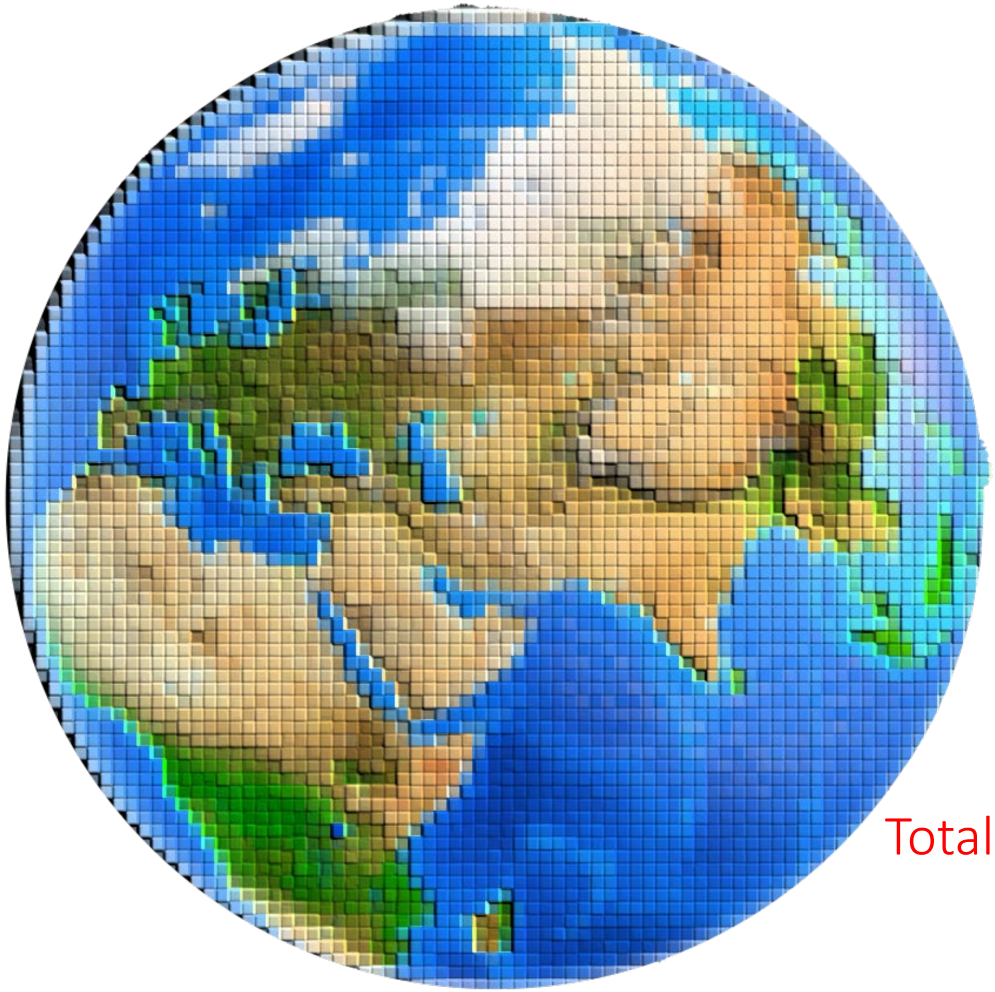

Run global UM model initialised from ECMWF analysis at grid-spacings of:

N96 (~130 km) Climate
N320 (~40 km) Seasonal

$$\tau_{Tot} = \tau_{RES} + \tau_{GWD}$$

Total momentum flux

Resolved momentum flux: $\overline{\rho u'w'}$

Parametrized momentum flux

Total momentum flux should be constant across resolutions

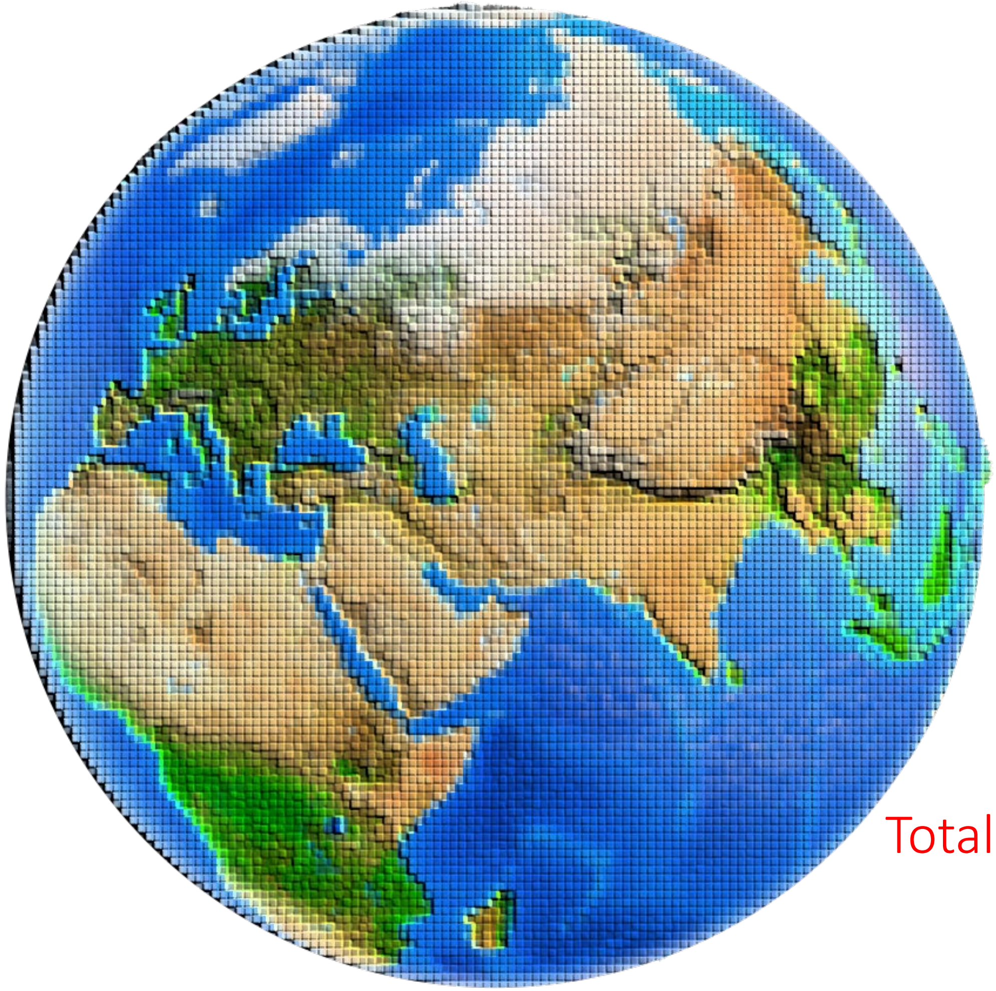

Run global UM model initialised from ECMWF analysis at grid-spacings of:

N96 (~130 km) Climate
N320 (~40 km) Seasonal
N1280 (~9 km) Global NWP

$$\tau_{Tot} = \tau_{RES} + \tau_{GWD}$$

Total momentum flux

Resolved momentum flux: $\overline{\rho u' w'}$

Parametrized momentum flux

Total momentum flux is smaller at lower resolutions

Resolved GW momentum flux

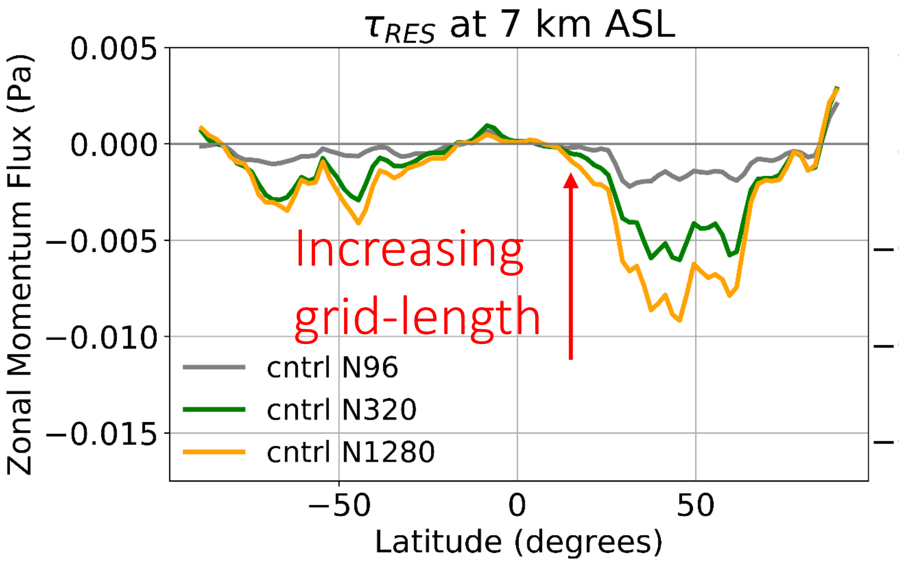

Resolved GW momentum flux decreases at larger grid-lengths

Parametrized GW momentum flux

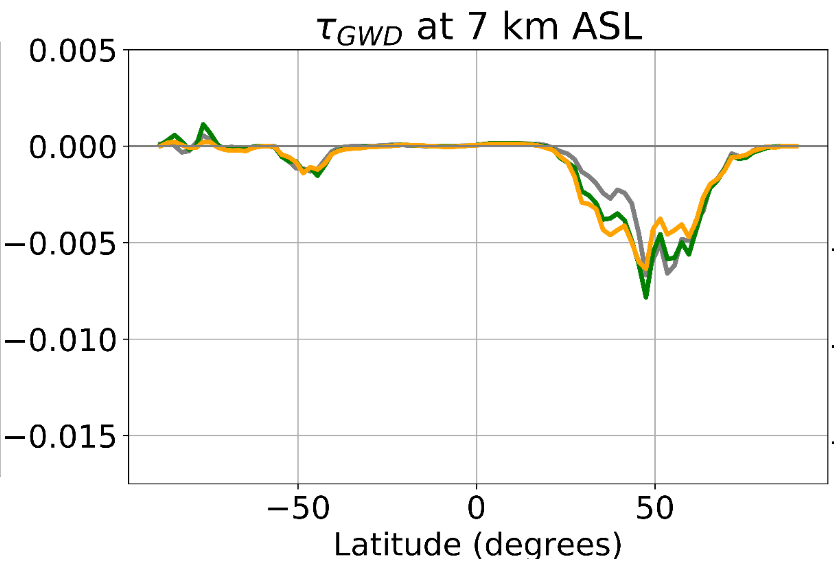

Parametrized GW momentum flux is almost insensitive to grid-length

Total GW momentum flux

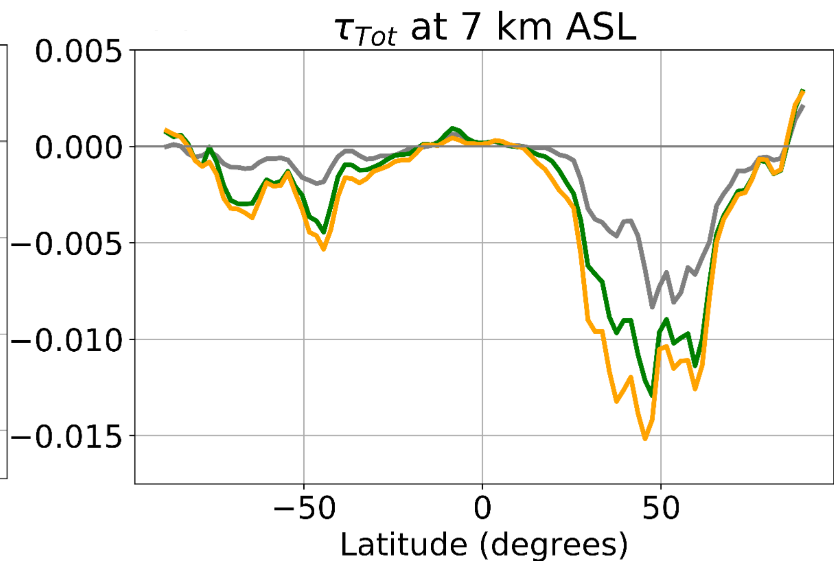

Total GW momentum flux is significantly underestimated at large grid-lengths

Plots show: zonal mean zonal gravity wave momentum fluxes at 7 km above sea level

Stratospheric winds are stronger at lower resolutions

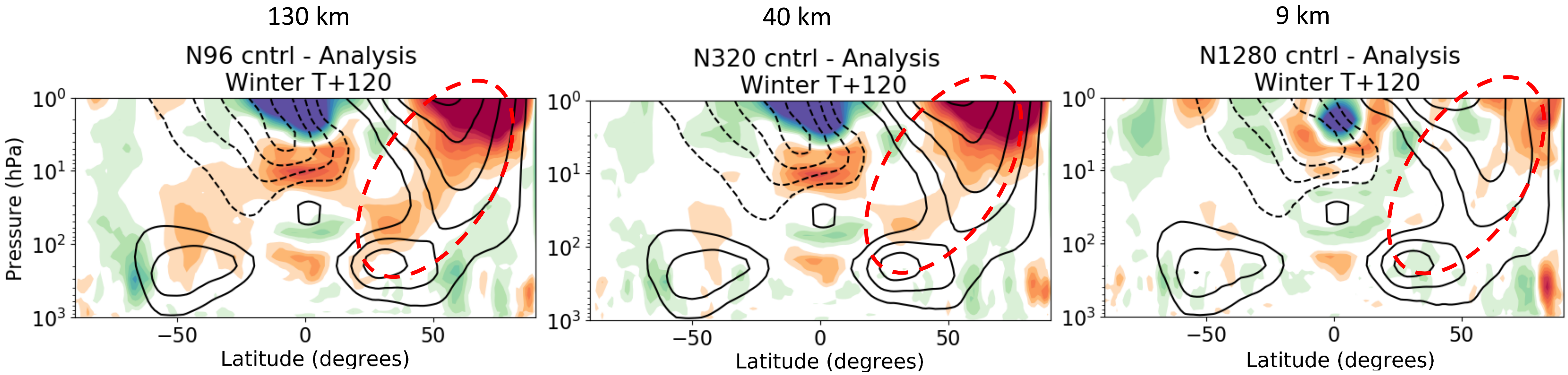

Plots show: zonal mean zonal wind error relative to analysis at lead time of 5 days

ECMWF

Total momentum flux is smaller at lower resolutions

Resolved GW momentum flux

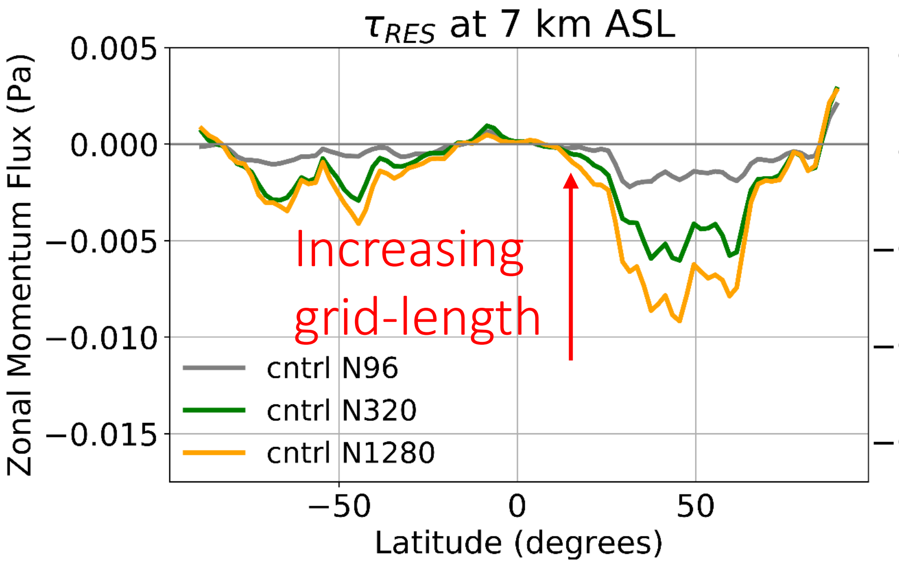

Parametrized GW momentum flux

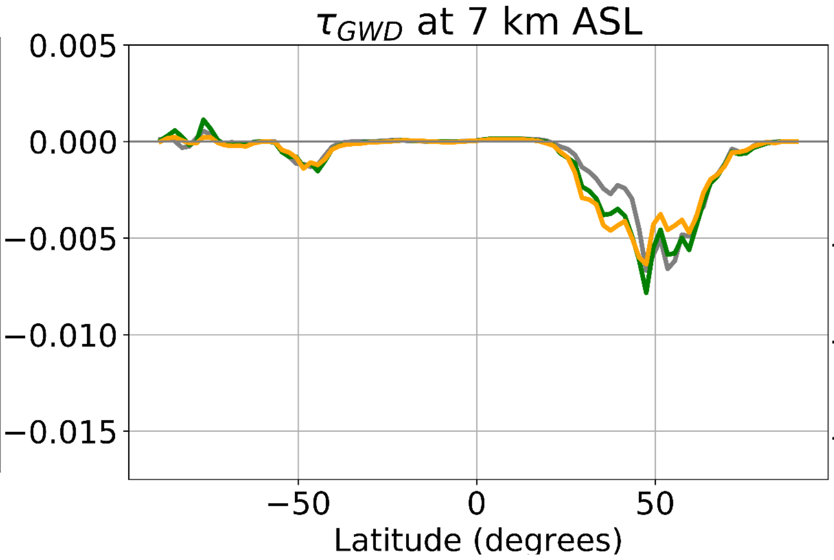

Total GW momentum flux

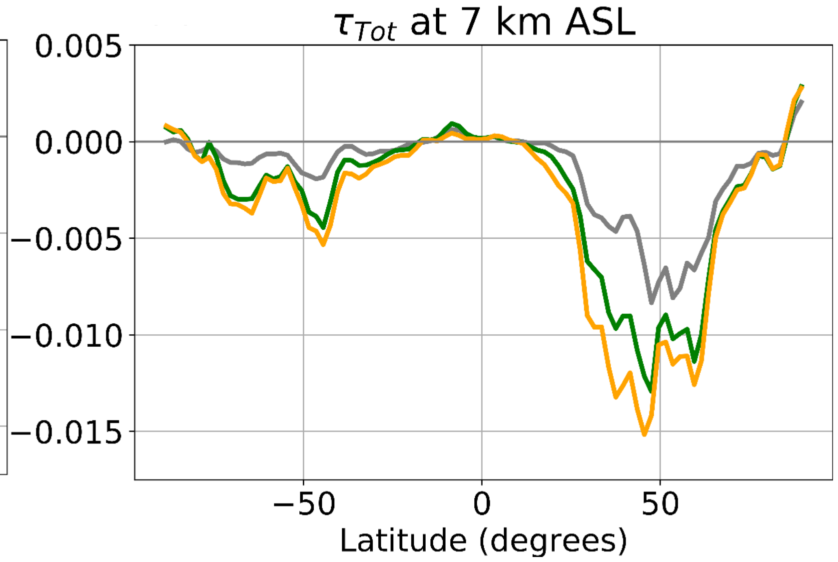

Resolved GW momentum flux decreases at larger grid-lengths

Parametrized GW momentum flux is almost insensitive to grid-length

Total GW momentum flux is significantly underestimated at large grid-lengths

Plots show: zonal mean zonal gravity wave momentum fluxes at 7 km above sea level

Parametrization

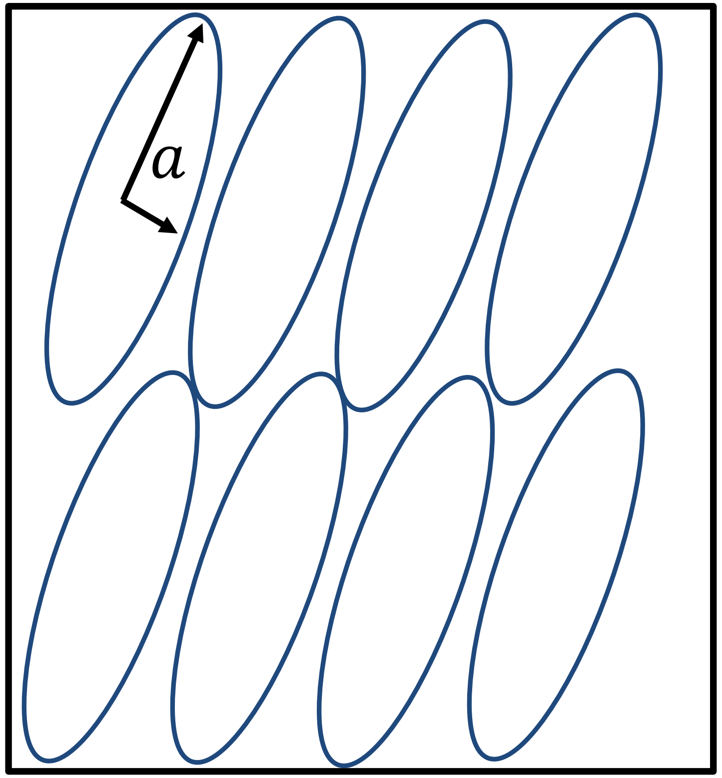

Reality

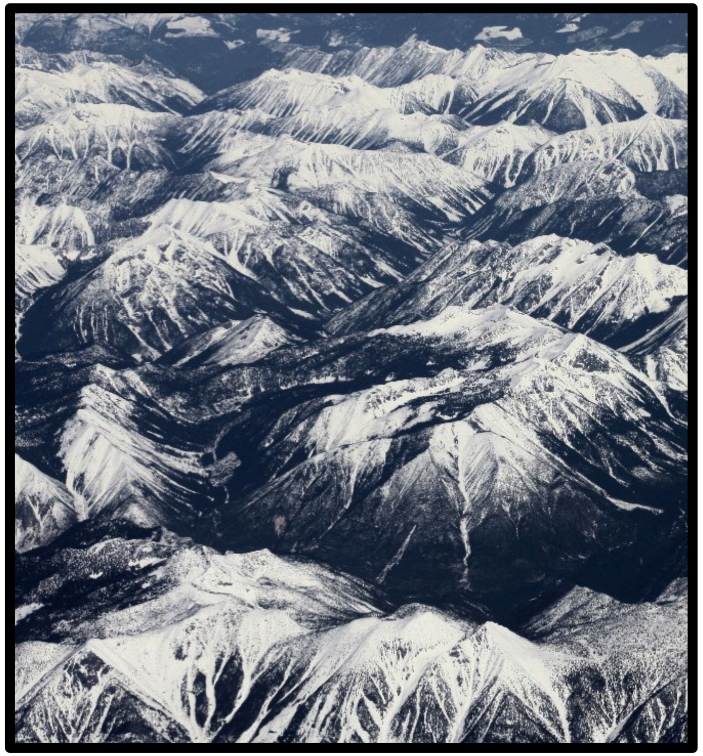

Single length-scale approximation is not entirely realistic

A more ‘scale-aware’ solution

Integrate over all subgrid scales

Hydrostatic linearised expression for orographic momentum flux at surface:

$$\tau_x, \tau_y = A^{-1}\rho_0 \int_{-\infty}^{\infty}\int_{-\infty}^{\infty}(u', v')w' dxdy$$

$$= A^{-1}\rho_0 N_o 4\pi^2 \int_{-\infty}^{\infty}\int_{-\infty}^{\infty}\frac{k,l}{K}(U_0 k + V_0 l)\left|\hat{h}\right|^2 dk\, dl$$

$\left|\hat{h}\right|$ = Fourier transform of surface height

See van Niekerk and Vosper (2021)

Integrate over all subgrid scales

Hydrostatic linearised expression for orographic momentum flux at surface:

$$\tau_x, \tau_y = A^{-1}\rho_0 \int_{-\infty}^{\infty}\int_{-\infty}^{\infty} (u', v')w' dxdy$$

$$= A^{-1}\rho_0 N_o 4\pi^2 \int_{-\infty}^{\infty}\int_{-\infty}^{\infty} \frac{k,l}{K}(U_0 k + V_0 l)\left|\hat{h}\right|^2 dk\, dl$$

$\left|\hat{h}\right|$ = Fourier transform of surface height

$$\tau_x, \tau_y = \rho_0 N_0 (U_0 F_1 + V_0 F_2, U_0 F_2 + V_0 F_3)$$

$$F_1 = A^{-1} 4\pi^2 \int_{l_{min}}^{l_{max}}\int_{k_{min}}^{k_{max}} \frac{k^2}{K}\left|\hat{h}\right|^2 dk\, dl$$

$$F_2 = A^{-1} 4\pi^2 \int_{l_{min}}^{l_{max}}\int_{k_{min}}^{k_{max}} \frac{kl}{K}\left|\hat{h}\right|^2 dk\, dl$$

$$F_3 = A^{-1} 4\pi^2 \int_{l_{min}}^{l_{max}}\int_{k_{min}}^{k_{max}} \frac{l^2}{K}\left|\hat{h}\right|^2 dk\, dl$$

Integrate over all wave directions and scales

See van Niekerk and Vosper (2021)

Integrate over all subgrid scales

Hydrostatic linearised expression for orographic momentum flux at surface:

$$\tau_x, \tau_y = A^{-1}\rho_0 \int_{-\infty}^{\infty}\int_{-\infty}^{\infty} (u', v')w' dxdy$$

$$= A^{-1}\rho_0 N_o 4\pi^2 \int_{-\infty}^{\infty}\int_{-\infty}^{\infty} \frac{k,l}{K}(U_0 k + V_0 l)\left|\hat{h}\right|^2 dk\, dl$$

$\left|\hat{h}\right|$ = Fourier transform of surface height

$$\tau_x, \tau_y = \beta\left(\frac{z_{blk}}{h_{amp}}\right)\rho_0 N_0 (U_0 F_1 + V_0 F_2, U_0 F_2 + V_0 F_3)$$

Accounts for flow blocking

See van Niekerk and Vosper (2021)

$$\left.\begin{aligned}
F_1 &= A^{-1}4\pi^2 \int_{l_{min}}^{l_{max}}\int_{k_{min}}^{k_{max}} \frac{k^2}{K}\left|\hat{h}\right|^2 dk\, dl \\
F_2 &= A^{-1}4\pi^2 \int_{l_{min}}^{l_{max}}\int_{k_{min}}^{k_{max}} \frac{kl}{K}\left|\hat{h}\right|^2 dk\, dl \\
F_3 &= A^{-1}4\pi^2 \int_{l_{min}}^{l_{max}}\int_{k_{min}}^{k_{max}} \frac{l^2}{K}\left|\hat{h}\right|^2 dk\, dl
\end{aligned}\right\}$$

Integrate over all wave directions and scales

Total momentum flux is more constant across resolutions

Resolved GW momentum flux

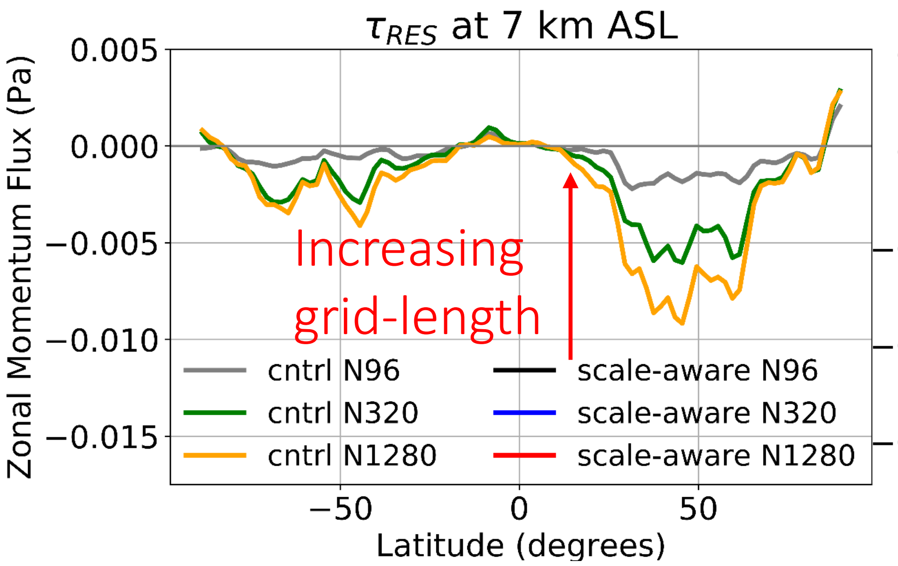

Resolved GW momentum flux decreases at larger grid-lengths

Parametrized GW momentum flux

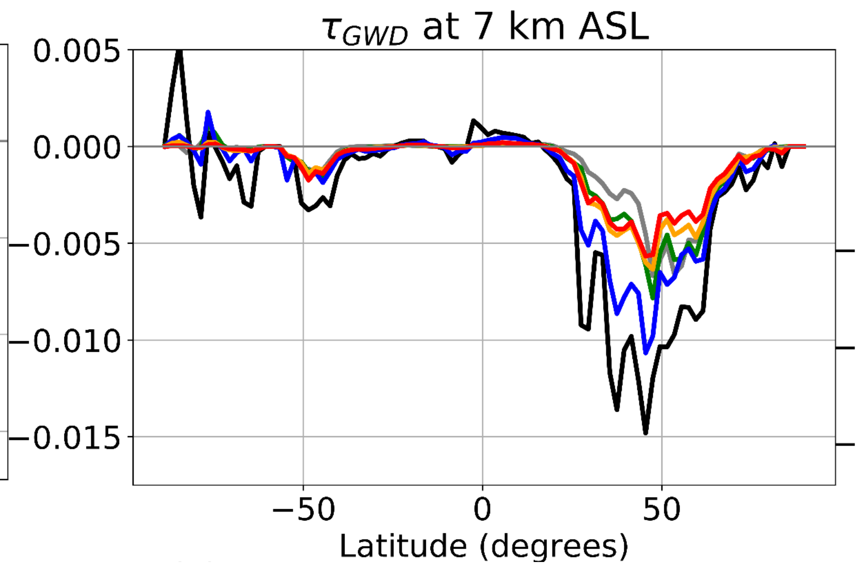

Parametrized GW momentum flux increases at larger grid-length

Total GW momentum flux

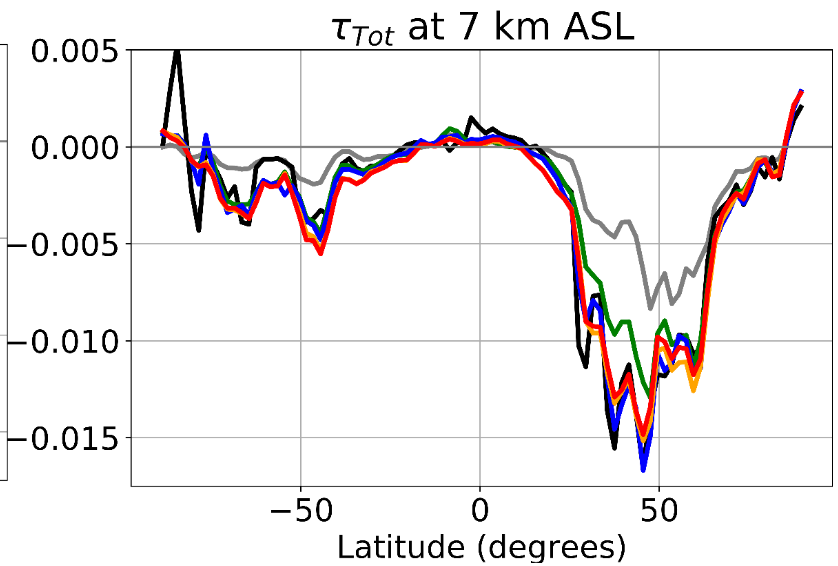

Total GW momentum flux is almost constant at different grid-lengths

Plots show: zonal mean zonal gravity wave momentum fluxes at 7 km above sea level

ECMWF

Improved stratospheric winds

130 km

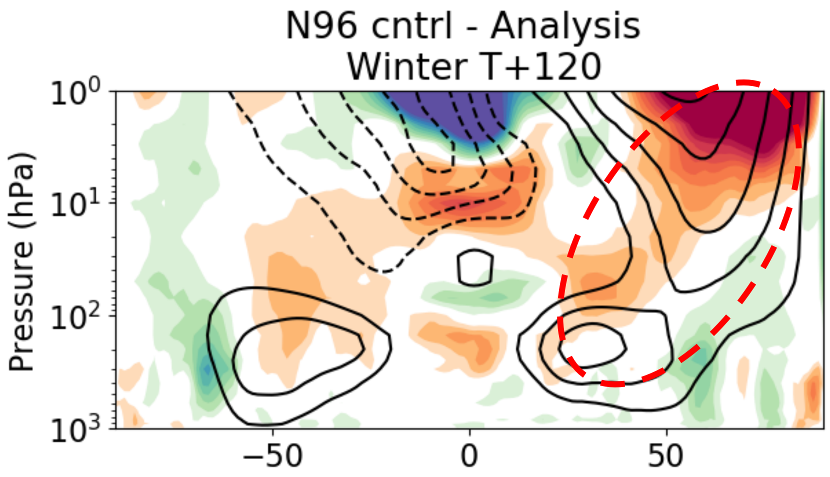

40 km

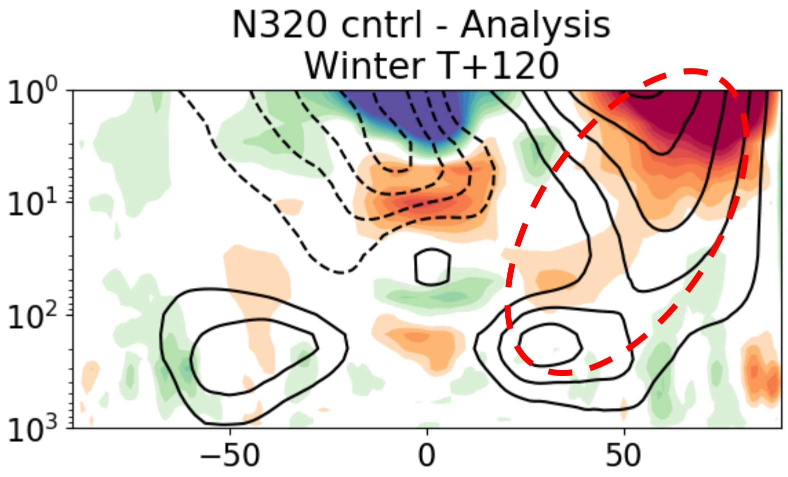

9 km

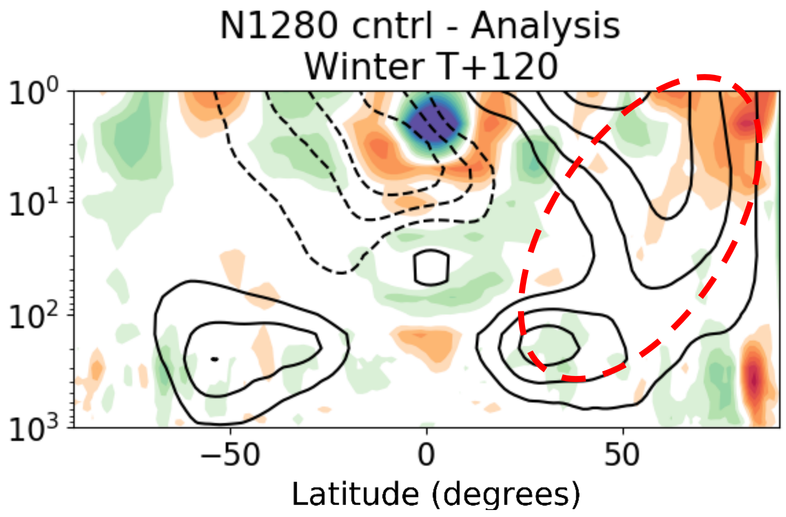

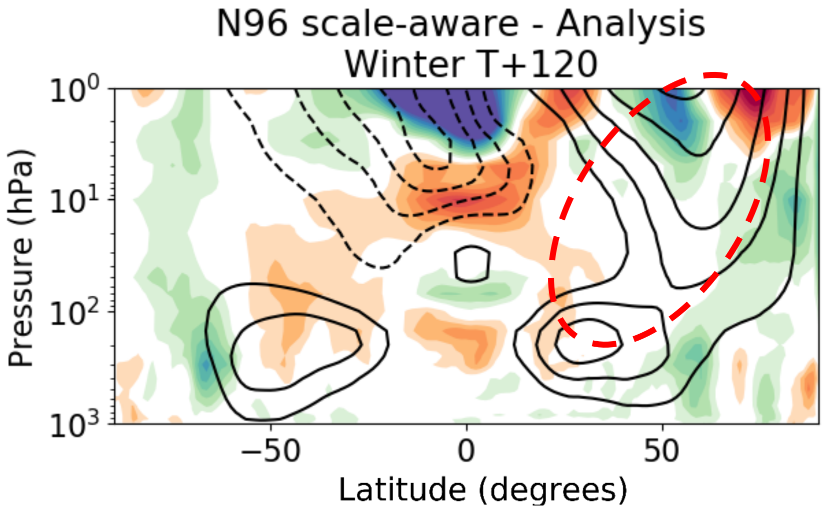

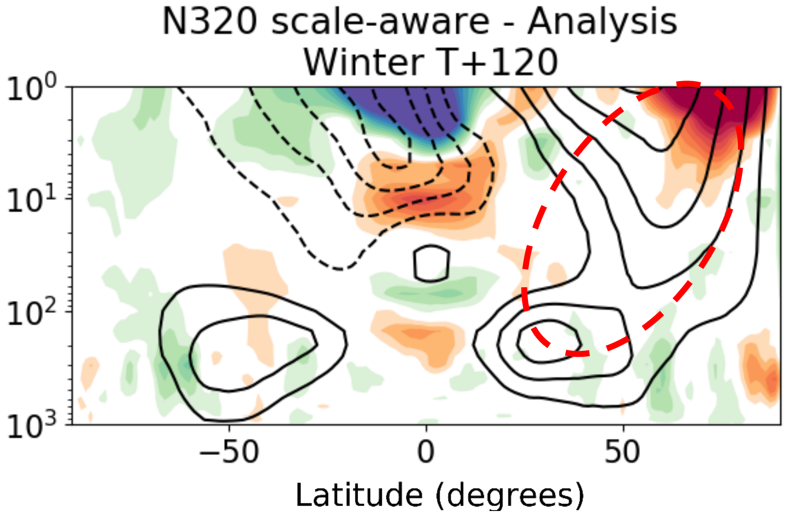

Day 5 error at N96 and N320 now much closer to that at N1280

Can we go further in representing mountain wave complexity?

Directional wind shear over complex orography

Complex orography

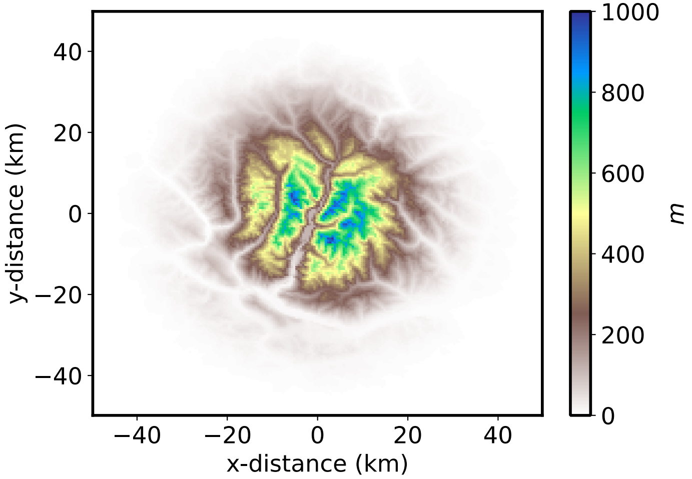

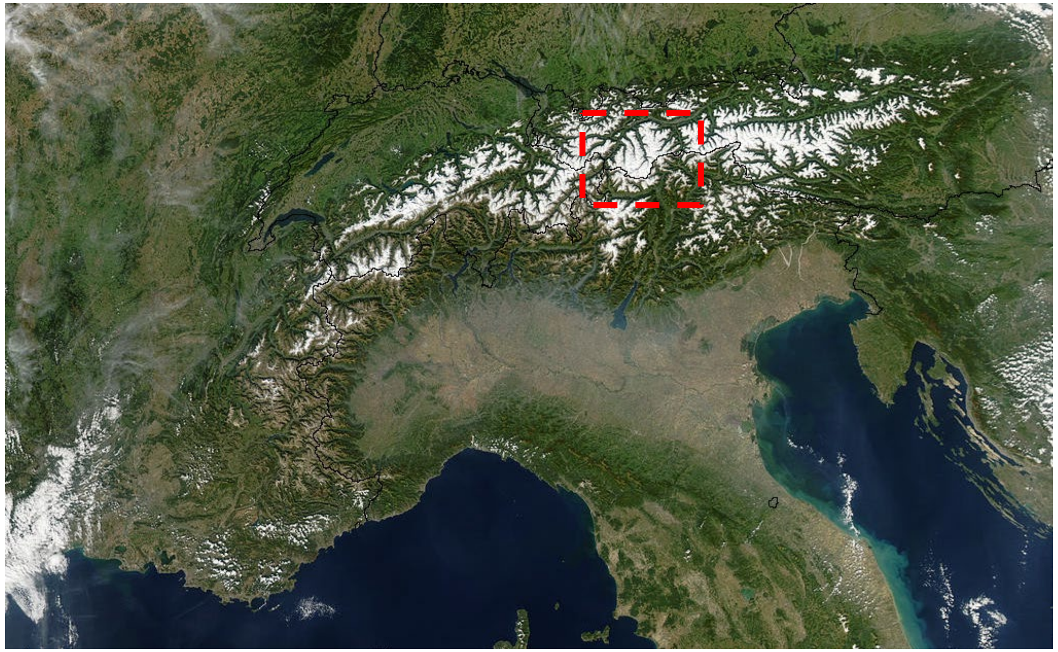

van Niekerk et al (2022), under review

Directional wind shear over complex orography

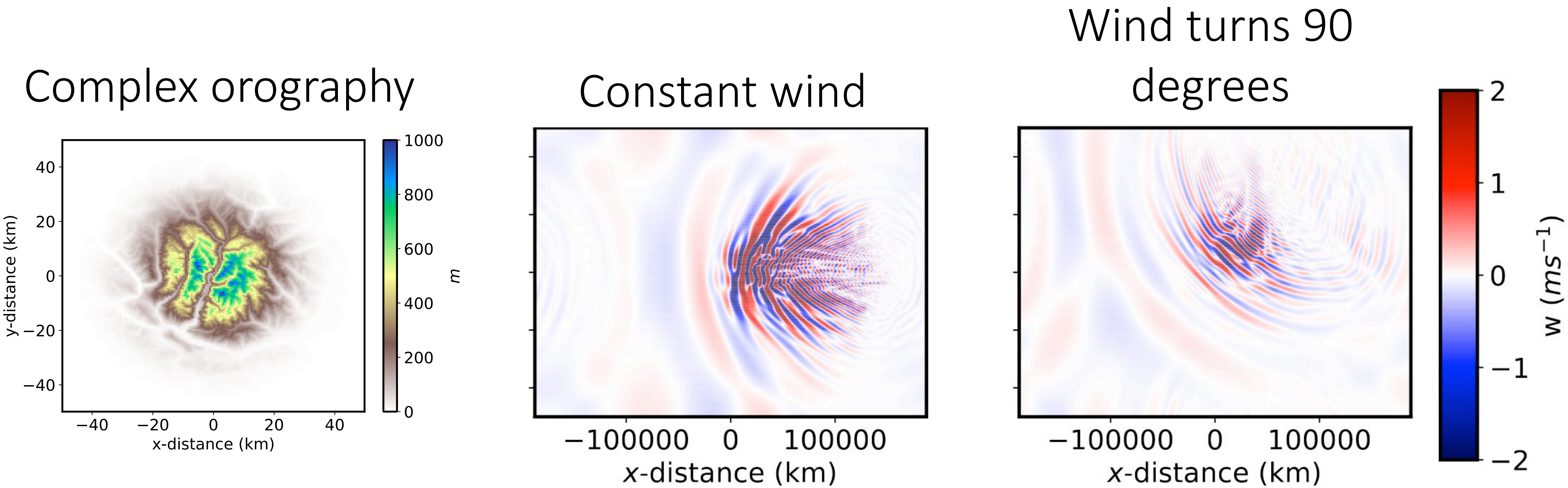

van Niekerk et al (2022), under review

Plots show vertical velocity at 22km in idealised simulations

What the current scheme does

$$\tau_x, \tau_y = \beta \left(\frac{z_{blk}}{h_{amp}} \right) \rho_0 N_0 [\, U_0 F_1 + V_0 F_2, U_0 F_2 + V_0 F_3 \,]$$

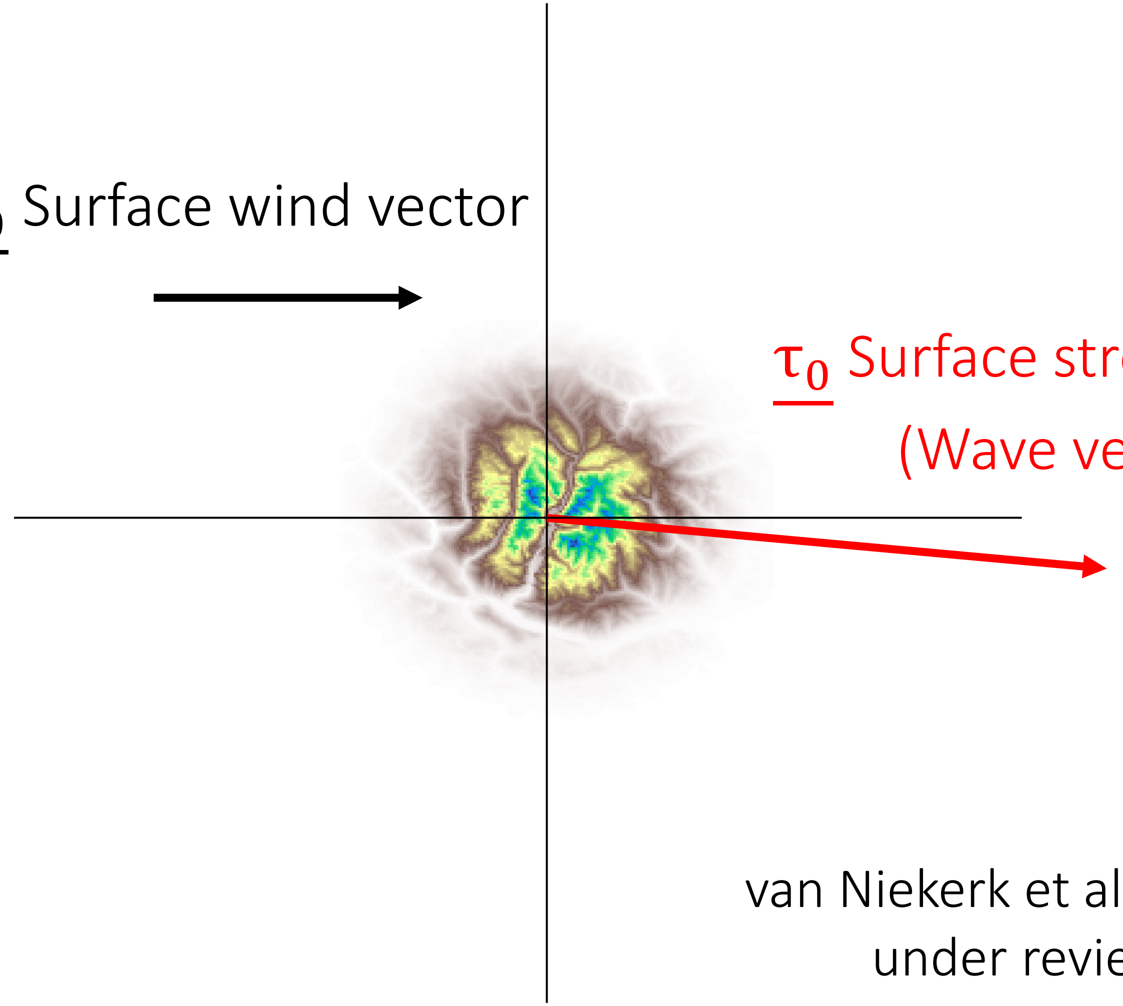

van Niekerk et al (2022), under review

What the current scheme does

$$\tau_x, \tau_y = \beta\left(\frac{z_{blk}}{h_{amp}}\right)\rho_0 N_0 [\, U_0 F_1 + V_0 F_2, U_0 F_2 + V_0 F_3 \,]$$

Saturation computed as:

When $\eta(z) > \frac{U}{N} F_{sat}$

U = wind in direction of wave vector

$U \rightarrow 0$ momentum deposited at one level

$\eta(z)$ = wave amplitude

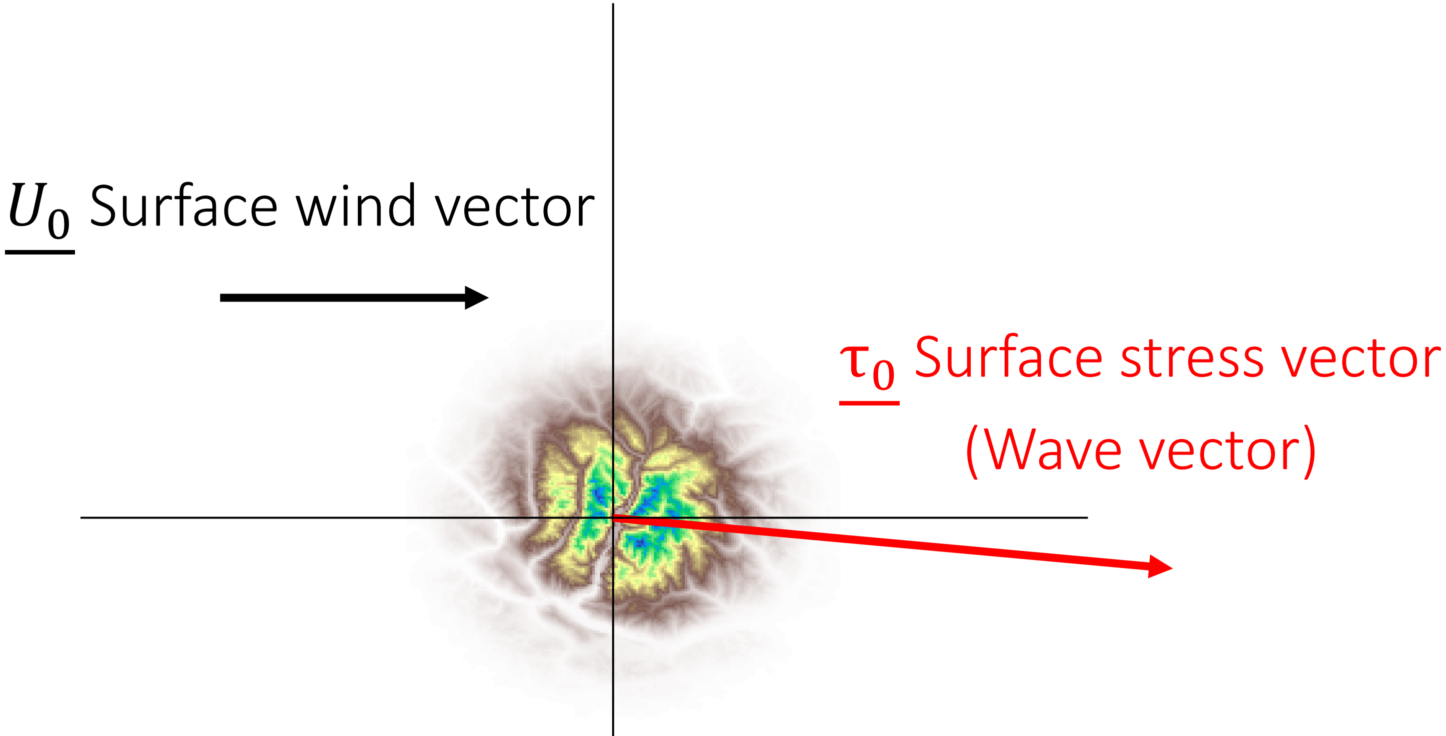

van Niekerk et al (2022), under review

What the current scheme does

$$\tau_x, \tau_y = \beta \left(\frac{z_{blk}}{h_{amp}} \right) \rho_0 N_0 [\, U_0 F_1 + V_0 F_2, U_0 F_2 + V_0 F_3 \,]$$

Saturation computed as:

When $\eta(z) > \frac{U}{N} F_{sat}$

$U\ =$ wind in direction of wave vector

$U\ \rightarrow 0$ momentum deposited at one level

$\eta(z)$ = wave amplitude

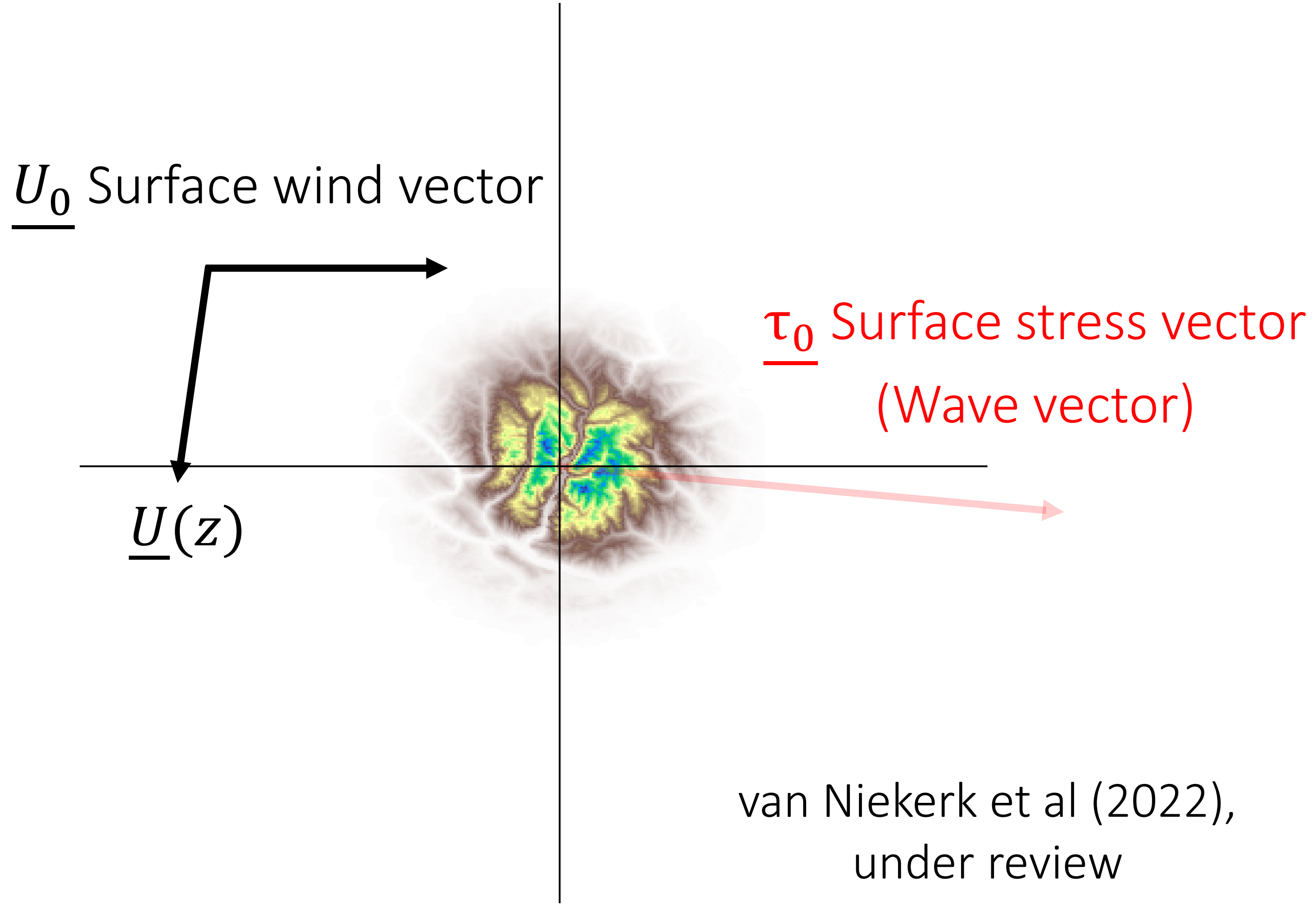

van Niekerk et al (2022), under review

What the directionally binned scheme does

$$\tau_x, \tau_y(\phi) = \beta \left(\frac{z_{blk}}{h_{amp}} \right) \rho_0 N_0 [\, U_0 F_1(\phi) + V_0 F_2(\phi), U_0 F_2(\phi) + V_0 F_3(\phi) \,]$$

ϕ = wave vector angle

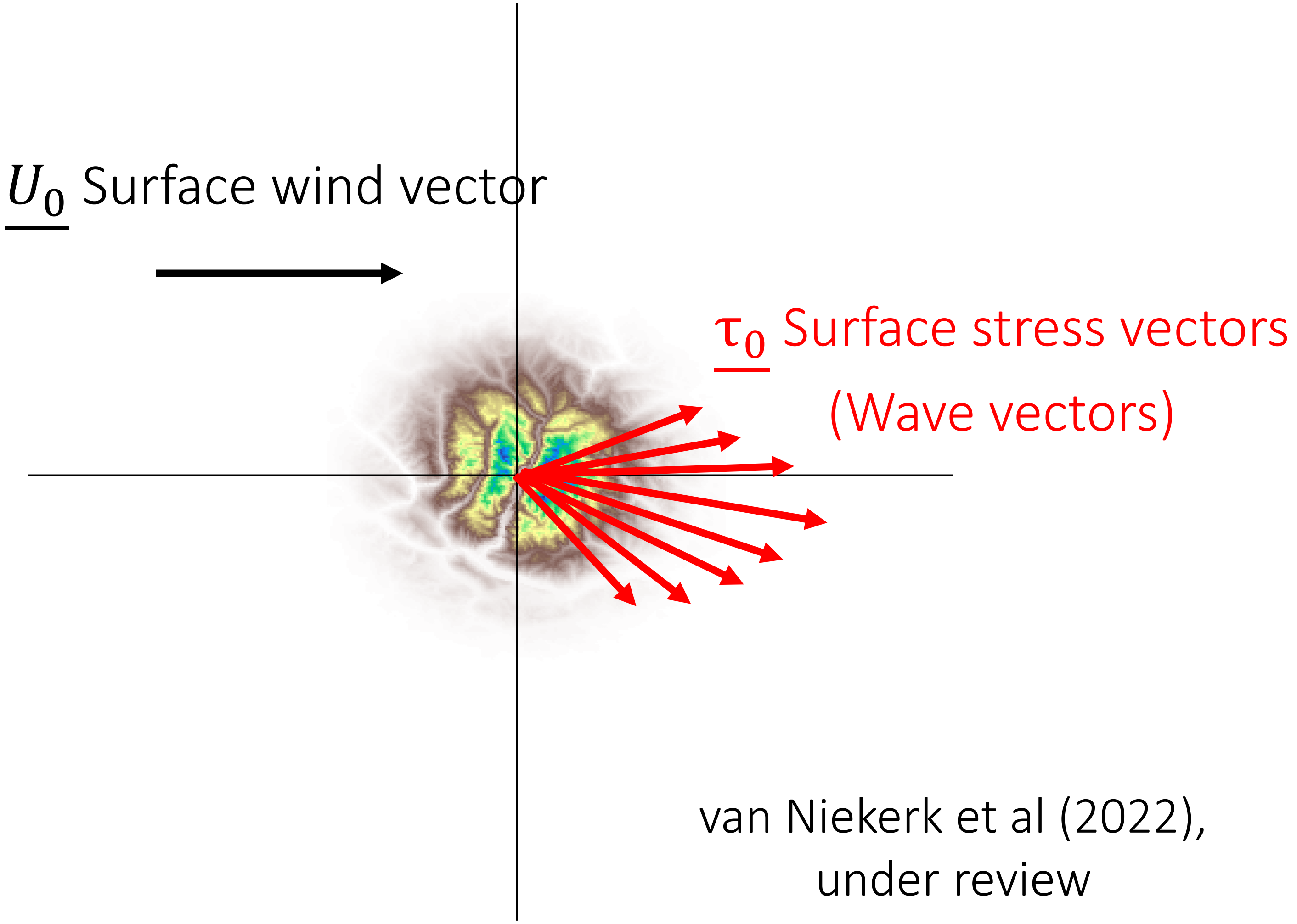

van Niekerk et al (2022), under review

What the directionally binned scheme does

$$\tau_x, \tau_y(\phi) = \beta \left(\frac{z_{blk}}{h_{amp}} \right) \rho_0 N_0 [\, U_0 F_1(\phi) + V_0 F_2(\phi), U_0 F_2(\phi) + V_0 F_3(\phi) \,]$$

ϕ = wave vector angle

Saturation computed as:

When $\eta(z,\phi) > \frac{U(\phi)}{N} F_{sat}$

$U(\phi) =$ wind in direction of wave vectors

$U(\phi) \rightarrow 0$ momentum deposited at corresponding level

$\eta(z)$ = wave amplitude in wave vector direction

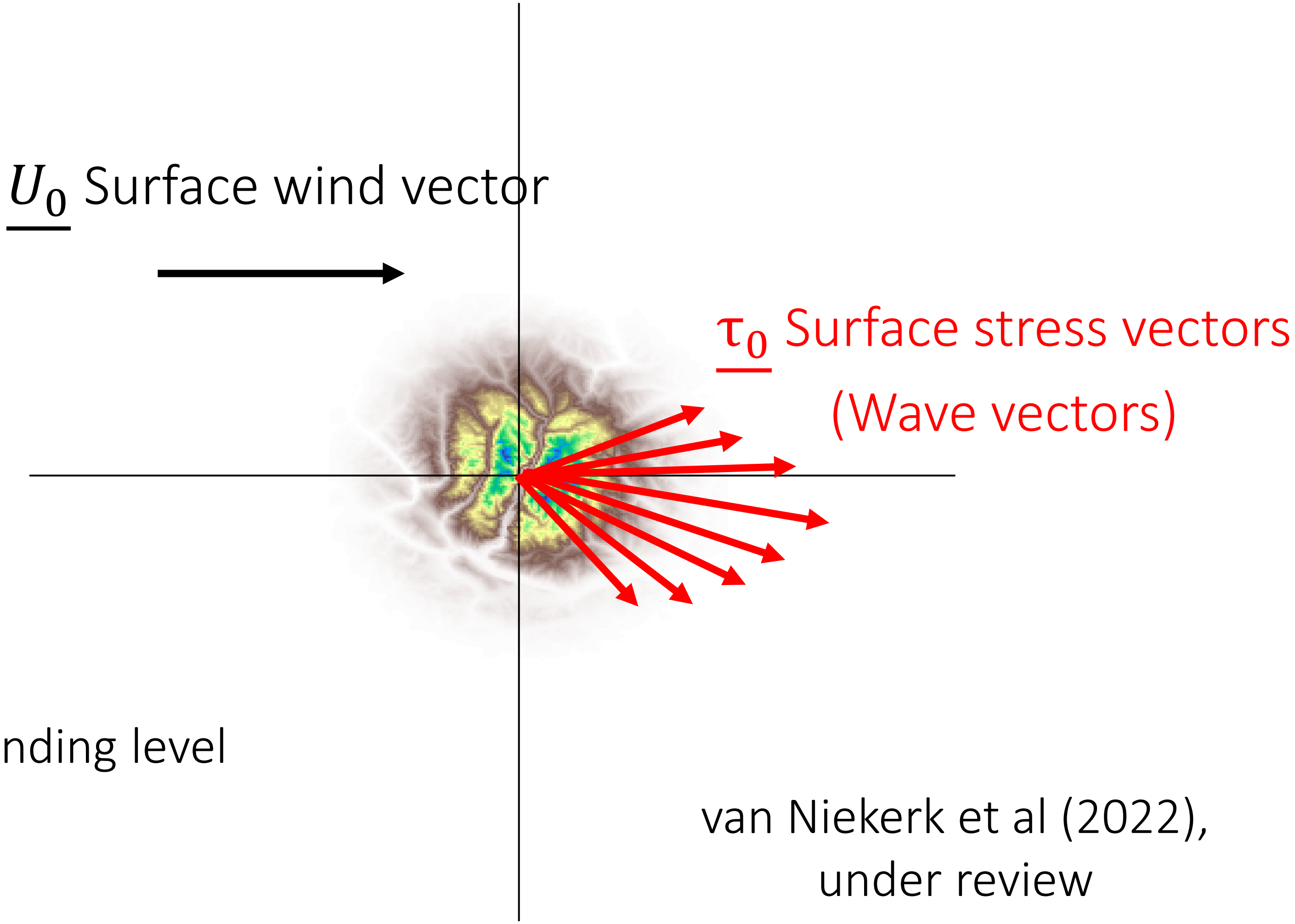

van Niekerk et al (2022), under review

What the directionally binned scheme does

$$\tau_x, \tau_y(\phi) = \beta \left(\frac{z_{blk}}{h_{amp}} \right) \rho_0 N_0 [\, U_0 F_1(\phi) + V_0 F_2(\phi), U_0 F_2(\phi) + V_0 F_3(\phi) \,]$$

ϕ = wave vector angle

Saturation computed as:

When $\eta(z,\phi) > \frac{U(\phi)}{N} F_{sat}$

$U(\phi) =$ wind in direction of wave vectors

$U(\phi) \rightarrow 0$ momentum deposited at corresponding level

$\eta(z)$ = wave amplitude in wave vector direction

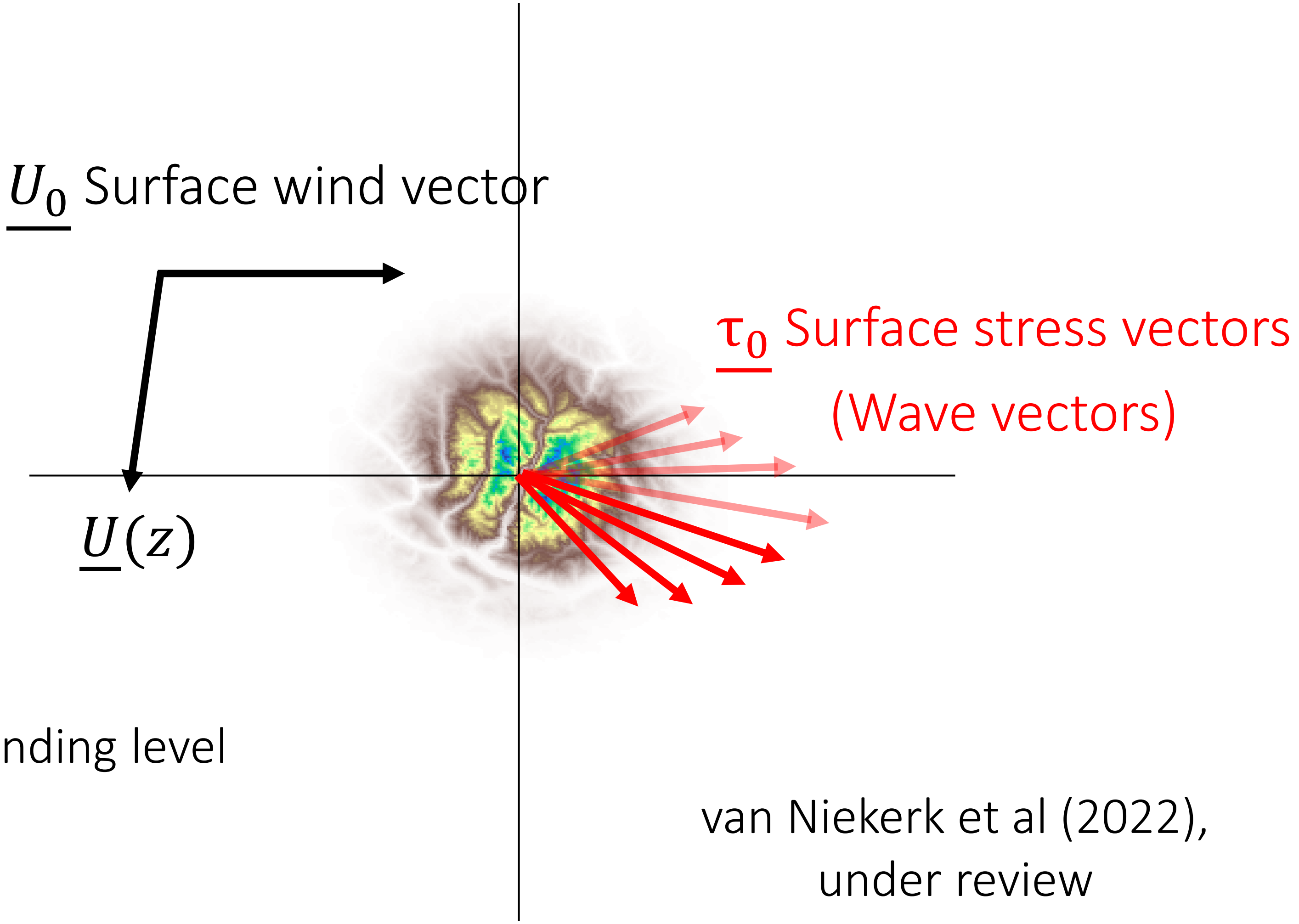

van Niekerk et al (2022), under review

What the directionally binned scheme does

Reduced gravity wave drag at lower altitudes

Increased gravity wave drag at higher altitudes

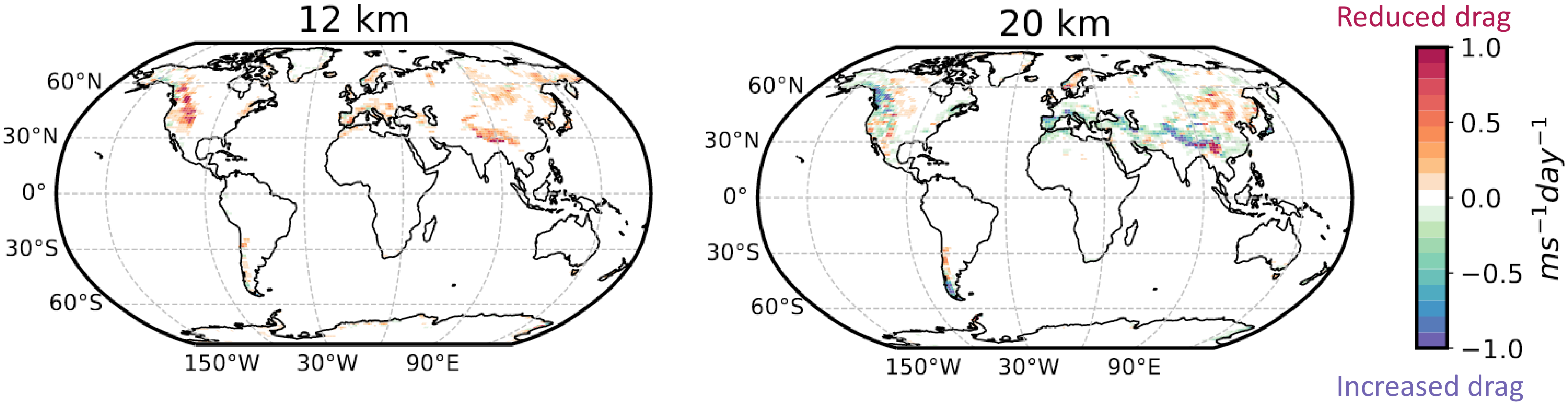

van Niekerk et al (2022), under review

ECMWF

Nonhydrostatic mountain waves are not represented at all (!)

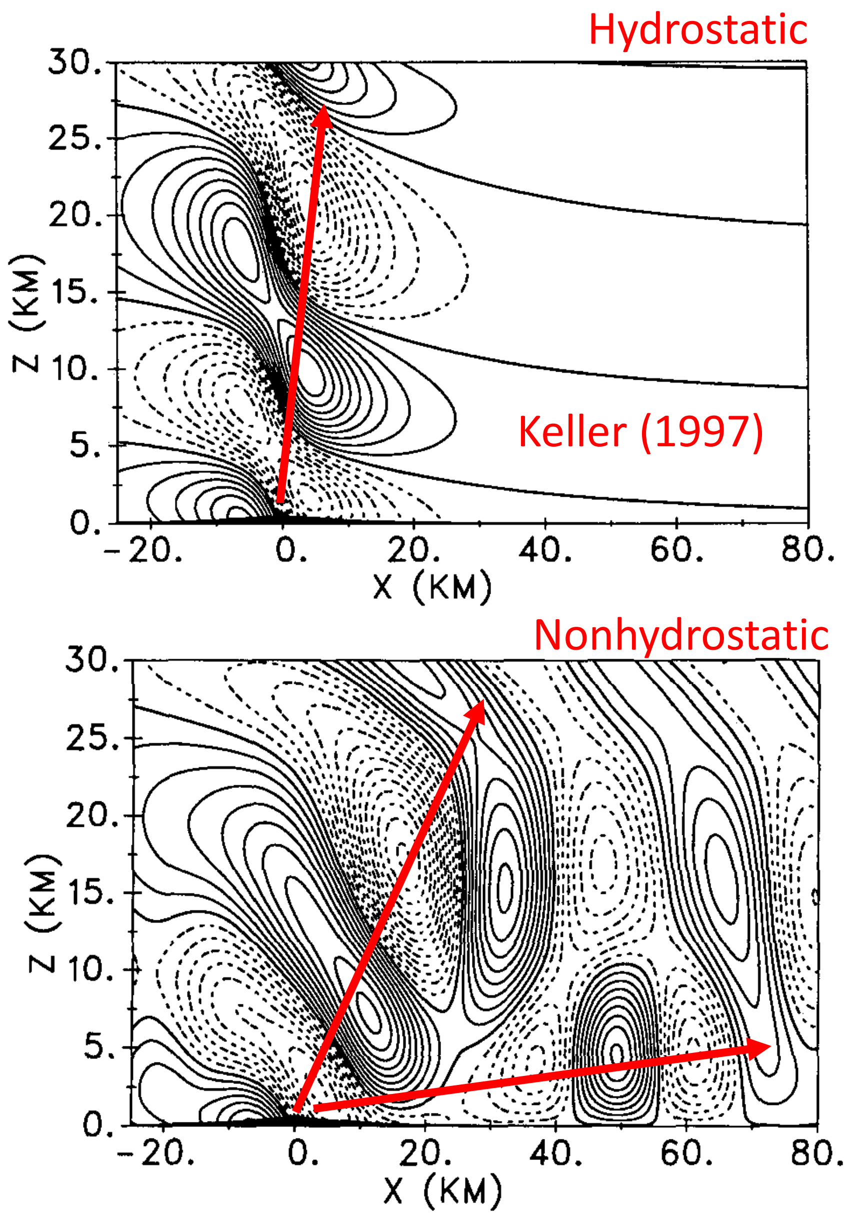

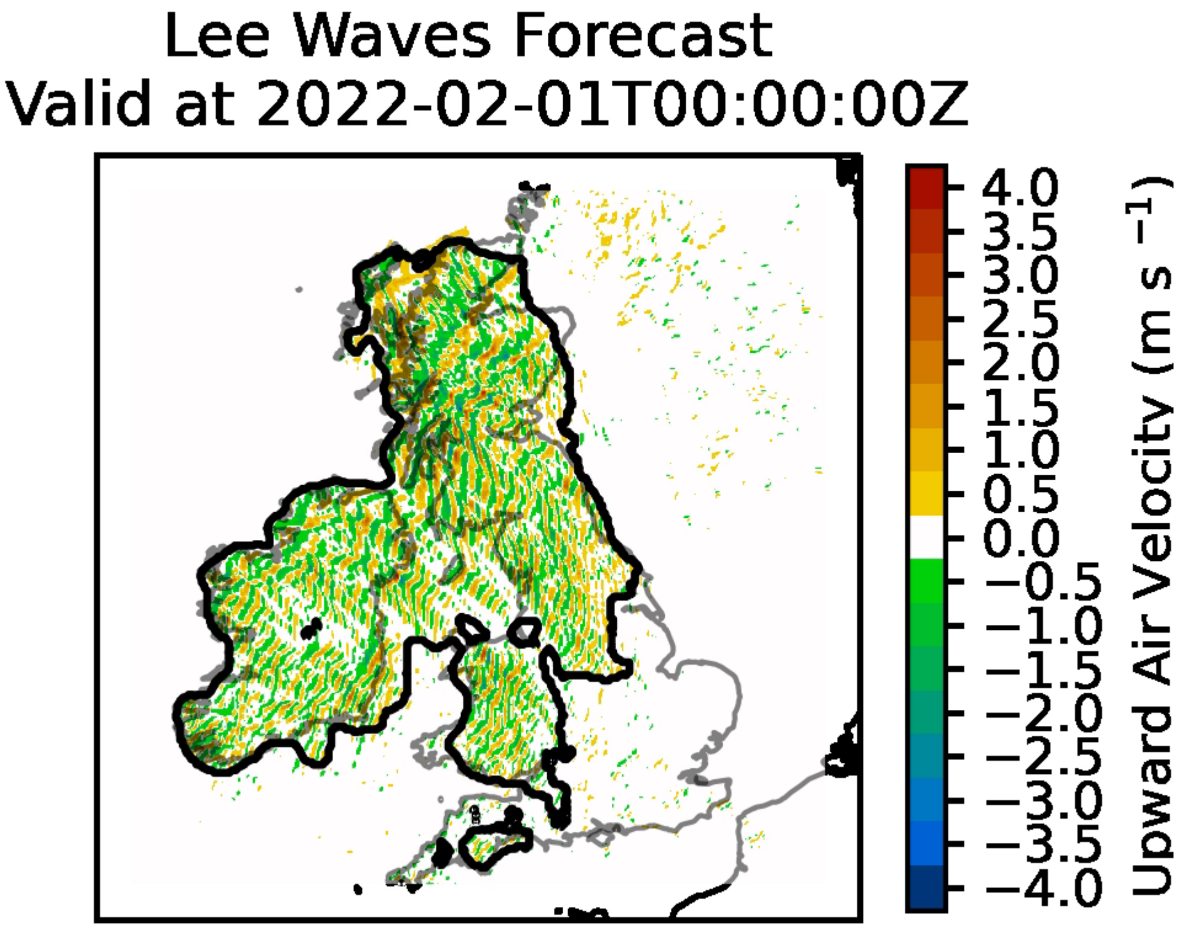

Animation c/o Jonathan Coney, Uni. Of Leeds

Current orographic gravity wave drag parametrizations assume that orography is made up of elliptical mountains within each grid-box – this means that the full range of subgrid scales are not represented

Representing the orography using Fourier transforms allows us to parametrize the subgrid orography more faithfully and across scales

This makes the gravity wave parametrization more ‘scale-aware’, and the total gravity wave flux more constant across grid-lengths - helping to improve the circulation in the stratosphere at coarser grid-lengths

By defining the subgrid orography using Fourier transforms, we are able to account for directional effects and the three-dimensional multi-scale nature of orography – perhaps even nonhydrostatic waves?

Current orographic gravity wave drag parametrizations assume that orography is made up of elliptical mountains within each grid-box – this means that the full range of subgrid scales are not represented

Representing the orography using Fourier transforms allows us to parametrize the subgrid orography more faithfully and across scales

This makes the gravity wave parametrization more 'scale-aware', and the total gravity wave flux more constant across grid-lengths - helping to improve the circulation in the stratosphere at coarser grid-lengths

By defining the subgrid orography using Fourier transforms, we are able to account for directional effects and the three-dimensional multi-scale nature of orography – perhaps even nonhydrostatic waves?

Current orographic gravity wave drag parametrizations assume that orography is made up of elliptical mountains within each grid-box – this means that the full range of subgrid scales are not represented

Representing the orography using Fourier transforms allows us to parametrize the subgrid orography more faithfully and across scales

This makes the gravity wave parametrization more ‘scale-aware’, and the total gravity wave flux more constant across grid-lengths - helping to improve the circulation in the stratosphere at coarser grid-lengths

By defining the subgrid orography using Fourier transforms, we are able to account for directional effects and the three-dimensional multi-scale nature of orography – perhaps even nonhydrostatic waves?

- Current orographic gravity wave drag parametrizations assume that orography is made up of elliptical mountains within each grid-box – this means that the full range of subgrid scales are not represented

- Representing the orography using Fourier transforms allows us to parametrize the subgrid orography more faithfully and across scales

- This makes the gravity wave parametrization more 'scale-aware', and the total gravity wave flux more constant across grid-lengths - helping to improve the circulation in the stratosphere at coarser grid-lengths

- By defining the subgrid orography using Fourier transforms, we are able to account for directional effects and the three-dimensional multi-scale nature of orography – perhaps even nonhydrostatic waves?